The Abdus Salam
International Centre for Theoretical Physics

United Nations
Educational, Scientific
and Cultural Organization

International Atomic
Energy Agency

SMR 1829 - 12

Winter College on Fibre Optics, Fibre Lasers and Sensors

12 - 23 February 2007

Spectroscopy of Rare Earth Doped Glasses

(part 2)

Anderson S. L. Gomes

Department of Physics
Universidade Federal de Pernambuco
Recife, PE, Brazil

Strada Costiera 11, 34014 Trieste, Italy - Tel. +39 040 2240 111; Fax +39 040 224 163 - sci_info@ictp.it, www.ictp.it

Spectroscopy of Rare Earth Doped Glasses

Lecture II

The Abdus Salam
International Centre for Theoretical Physics

United Nations
Educational, Scientific
and Cultural Organization

International Atomic
Energy Agency

Winter College on Fibre Optics, Fibre Lasers and Sensors
(12 - 23 February 2007)

Anderson S. L. Gomes
anderson@df.ufpe.br

Department of Physics
Universidade Federal de Pernambuco
Recife, PE, Brazil

Spectroscopy of Rare Earth Doped Glasses

Lessons Plan

Part II – Upconversion spectroscopy and Applications of REDG

II.1 Up-conversion Spectroscopy
II.2 REDG Ceramics
Applications of REDG
II.3 REDG for Lasers
II.4 REDG for Fiber Lasers and Amplifiers
II.5 REDG Planar and Channel Waveguides
II.6 REDG Microbarcodes

Literature

Upconversion spectroscopy

Chem. Rev. **2004,** *104,* 139–173 **139**

Upconversion and Anti-Stokes Processes with f and d Ions in Solids

François Auzel

GOTR, UMR 7574-CNRS, 1, Place A-Briand, 92195 Meudon Cedex, France

II.1 Upconversion Spectroscopy

Upconversion

Making 1x blue out of 2x red

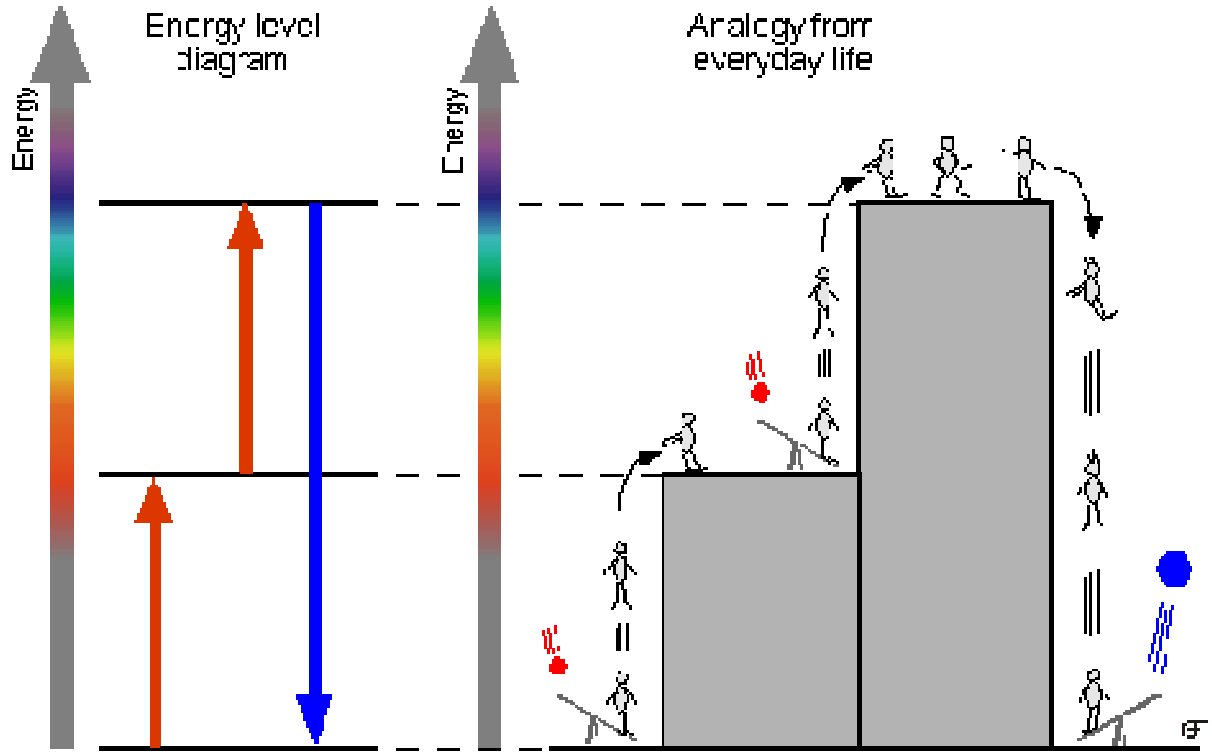

Energy Transfer

Chemical Reviews, 2004, Vol. 104, No. 1 **141**

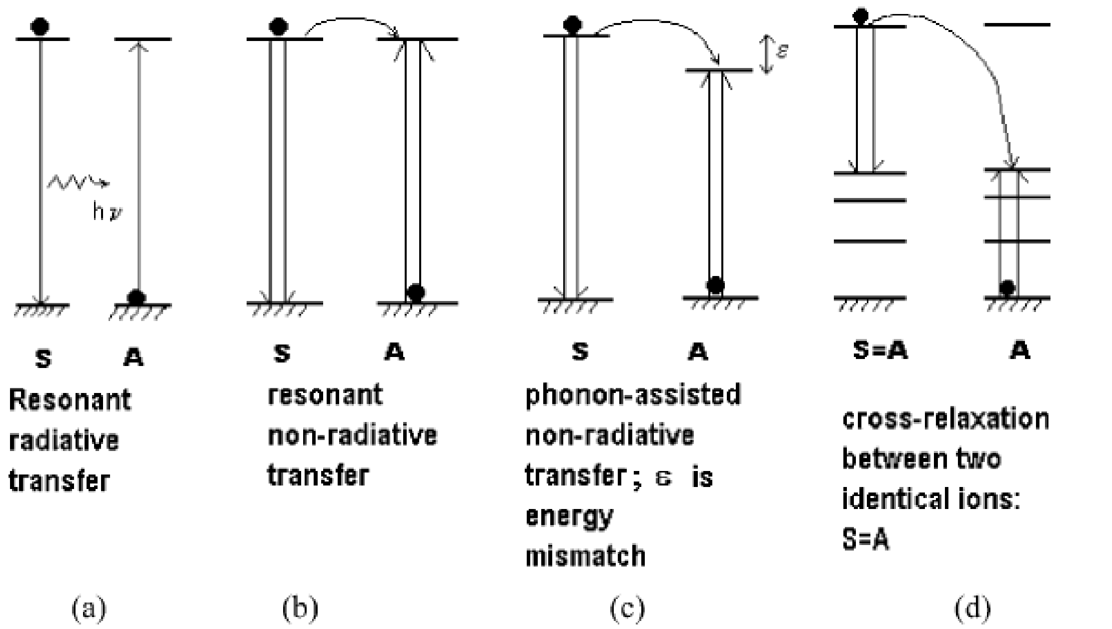

Figure 1. Various basic energy transfer processes between two ions considered before 1966: note that activator ion (A) receiving the energy from the sensitizer (S) is initially in its ground state. Cross-relaxation is the special case where S is identical to A. Doubled arrows symbolize the Coulombic interaction: (a) radiative resonant transfer; (b) resonant nonradiative transfer; (c) phonon-assisted nonradiative transfer; (d) cross-relaxation special case of nonradiative transfer.

Probability for such transfer between two ions at a sufficiently large distance R is found to be[20]

$$p_{SA}(R) = \frac{\sigma_A}{4\pi R^2} \frac{1}{\tau_S} \int g_S(\nu) g_A(\nu)\, d\nu \qquad (1)$$

R^{-2} dependence allows long range energy diffusion

$\longrightarrow$ photon trapping effects

Photon trapping increases apparent experimental lifetime!

II.1 Upconversion Spectroscopy

Let us take as example case 1(b)

For dipole-dipole interaction, the transfer probability can be written as (Förster, 1948) :

$$p_{SA} = \frac{1}{\tau_S}\left(\frac{R_0}{R}\right)^6$$

(Dexter, 1953)

The energy transfer probability for electric multipolar interactions can be more generally written as[27]

$$p_{SA} = \frac{(R_0/R)^s}{\tau_S} \qquad (4)$$

where s is a positive integer taking the following values:

$s = 6$ for dipole–dipole interactions,
$s = 8$ for dipole–quadrupole interactions,
$s = 10$ for quadrupole–quadrupole interactions.

Mechanisms for upconversion

Single ion resonant processes

(a) Sequential TPA (Two photon absorption) (or more!)
(b) SHG (second harmonic generation)
(c) TPA

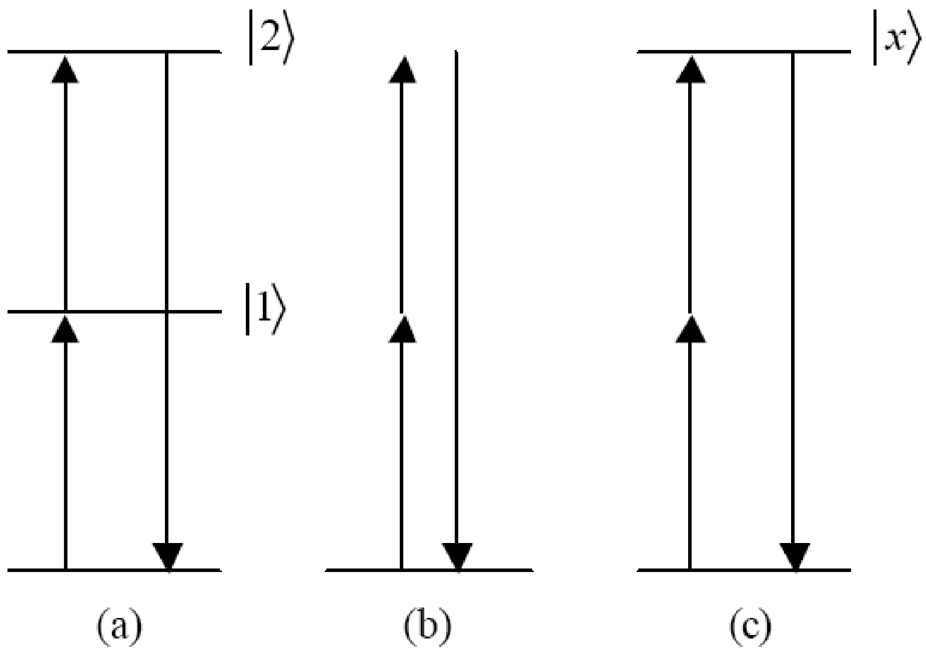

Two ions resonant processes

II.1 Upconversion Spectroscopy

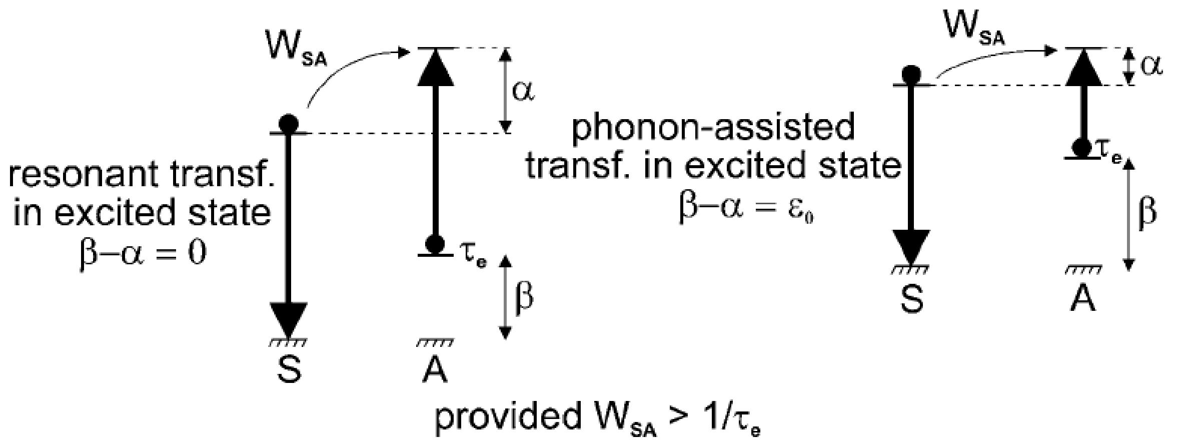

Figure 2. APTE basic step: energy transfer toward an ion already in an excited state. Nonradiative energy transfer is either resonant or phonon-assisted with energy mismatch $\epsilon_0 \neq 0$.

II.1 Upconversion Spectroscopy

Two photon upconversion processes efficiencies

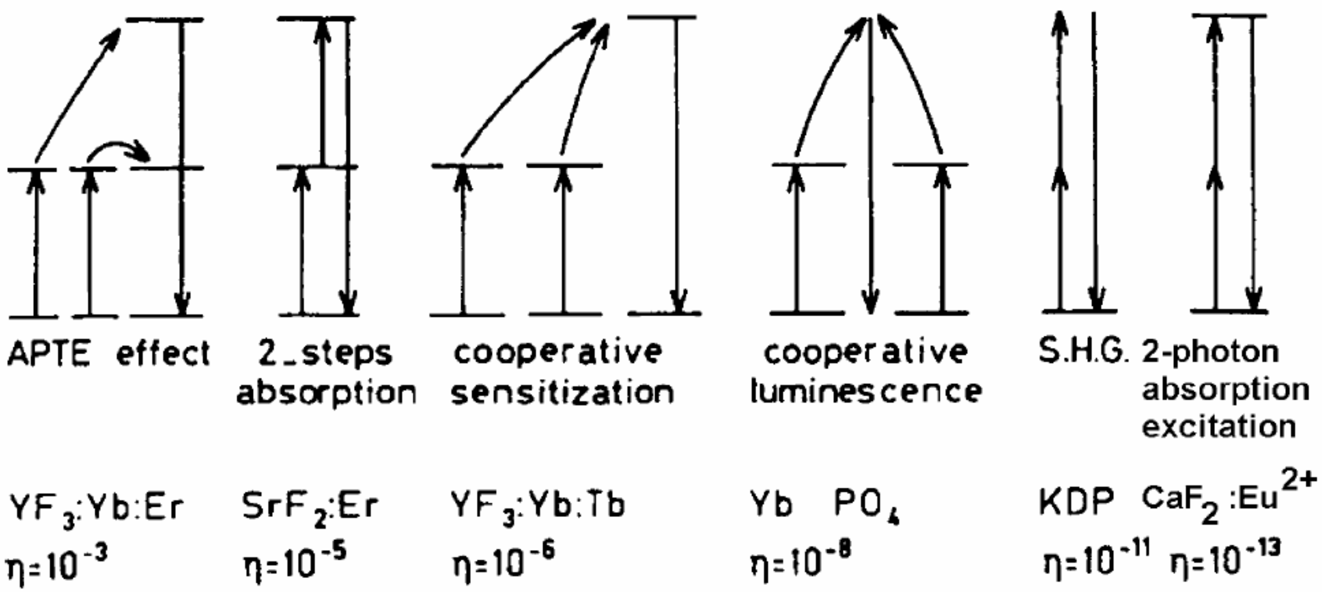

Figure 3. Various two-photon upconversion processes with their relative efficiency in considered materials.

II.1 Upconversion Spectroscopy

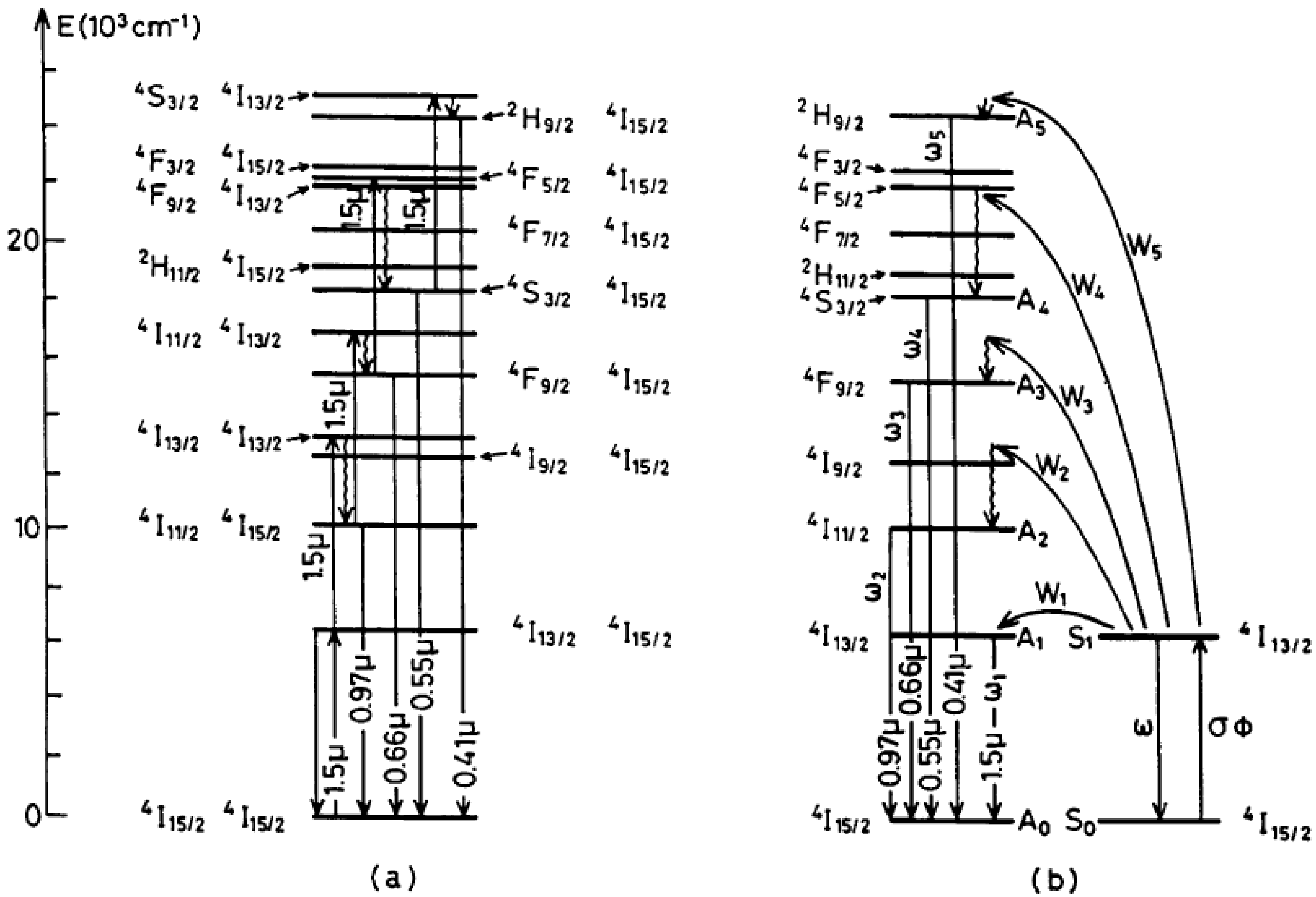

Figure 5. Cooperative (a) and APTE (b) energy scheme for n-photon ($n = 1-5$) upconversion in Er^{3+}-doped hosts.

II.1 Upconversion Spectroscopy

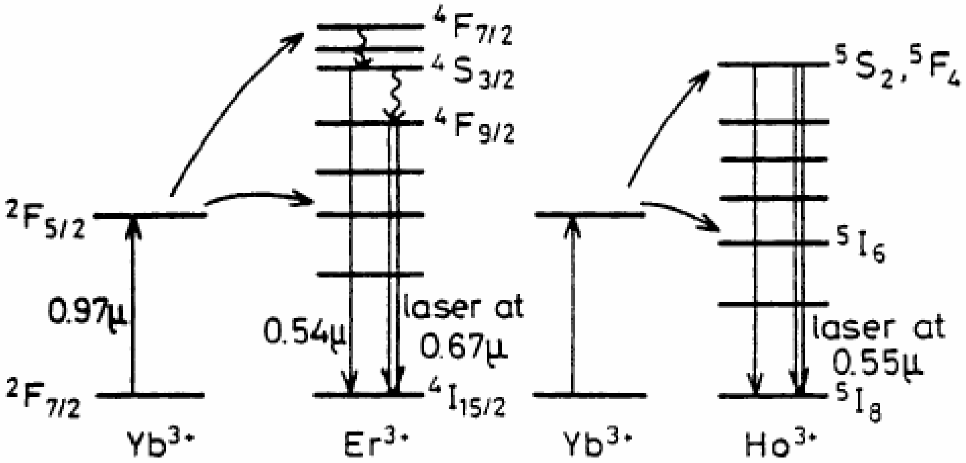

Figure 20. First operating APTE upconversion pulsed laser-pumping schemes in Yb–Ho and Yb–Er couples. (Reprinted with permission from ref 218. Copyright 1971 American Institute of Physics.)

IR pumped upconversion in thulium doped fiber

II.1 Upconversion Spectroscopy

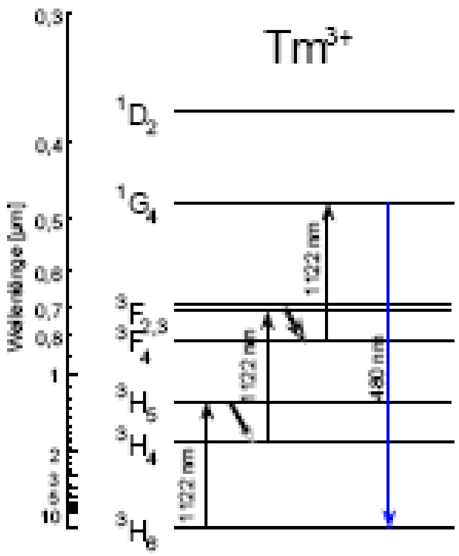

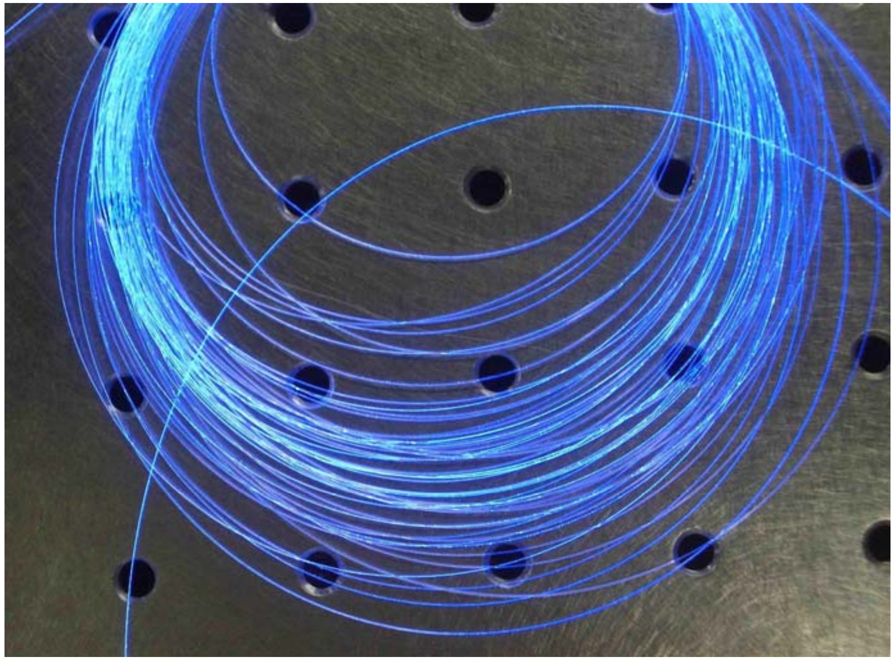

Cross relaxation

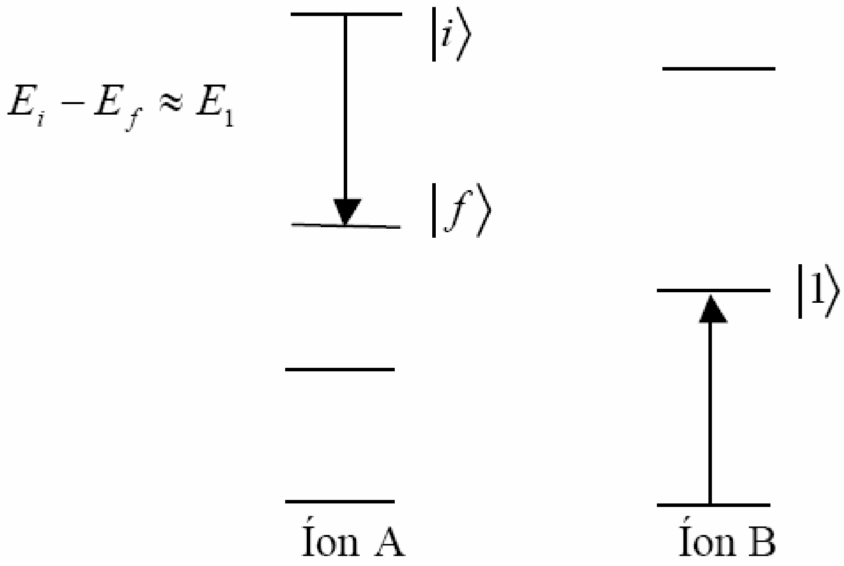

- Leads to FLUORESCENCE QUENCHING

- Strong dependence on ions concentration

II.1 Upconversion Spectroscopy

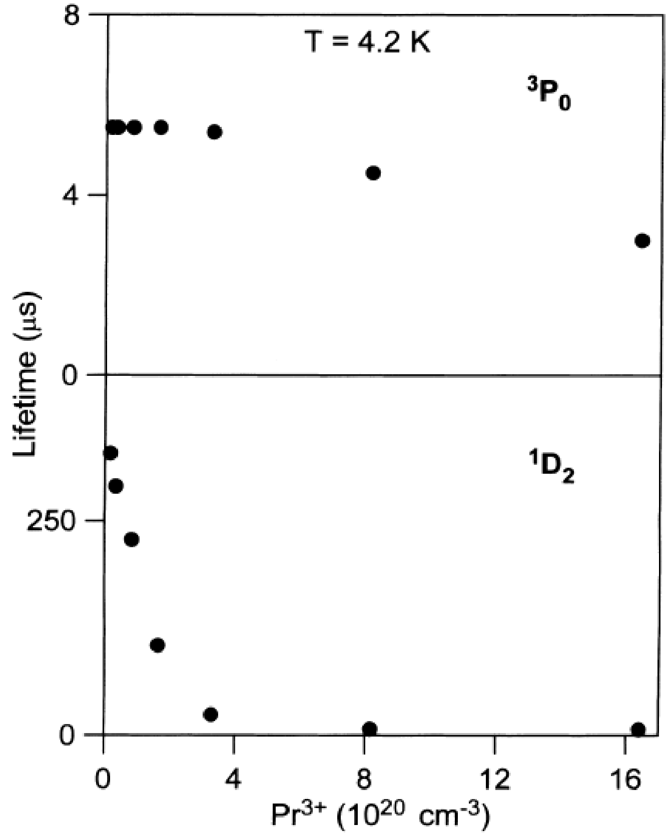

Fig. 6. Lifetime values of $^3P_0$ and $^1D_2$ levels as a function of concentration at 4.2 K. Lifetimes were obtained by exciting at 486 nm and collecting the luminescence at 525 and 606 nm, respectively.

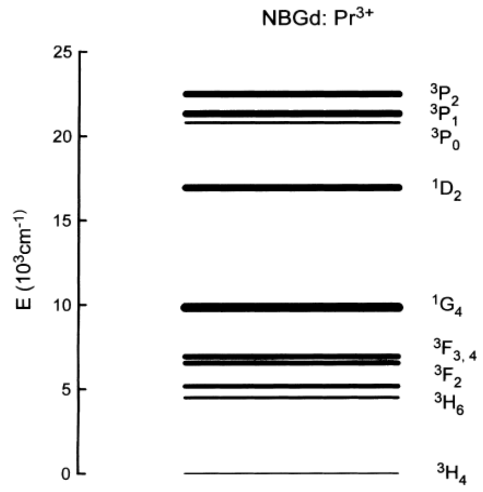

Fig. 2. Energy levels diagram of Pr^{3+} in NBGd fluorophosphate glass (from the absorption data).

5. Conclusions

From the above results, the following conclusions can be reached:

1. Fluorescence quenching from the $^1D_2$ state has been demonstrated to occur for Pr^{3+} concentrations higher than 0.1 mol% even at 4.2 K. This can be attributed to a cross relaxation process.
2. The time evolution of the decays from the $^1D_2$ state for concentrations higher than 0.1 mol% is consistent with a dipole–dipole energy transfer mechanism.

R. Balda, Fernándeza, I. Saéz de Ocáriza, J. L. Adam, A. Mendioroz and E. Montoya
Opt. Mat. 13, 159-165 (1999)

II.1 Upconversion Spectroscopy

Available online at www.sciencedirect.com

ScienceDirect

Journal of Non-Crystalline Solids 352 (2006) 3636–3641

JOURNAL OF NON-CRYSTALLINE SOLIDS

www.elsevier.com/locate/jnoncrysol

1.5 μm Emission and infrared-to-visible frequency upconversion in Er^{+3}/Yb^{+3}-doped phosphoniobate glasses

A.J. Barbosa [a], F.A. Dias Filho [a], Y. Messaddeq [a], S.J.L. Ribeiro [a,*], R.R. Gonçalves [b], S.R. Lüthi [c], A.S.L. Gomes [c]

[a] *Instituto de Química – UNESP, Departamento de Quimica Geral e, CP 355, Araraquara-SP 14801-970, Brazil*

[b] *Departamento de Química, Faculdade de Filosofia, Ciências e Letras de Ribeirão Preto, USP, Ribeirão Preto-SP, 14040-901, Brazil*

[c] *Departamento de Física, UFPE, Recife-PE, 50670-901, Brazil*

Available online 24 July 2006

Abstract

Sodium phosphoniobate glasses with the composition (mol%) $75NaPO_3$–$25Nb_2O_5$ and containing 2 mol% Yb^{3+} and x mol% Er^{3+} ($0.01 \leqslant x \leqslant 2$) were prepared using the conventional melting/casting process. Er^{3+} emission at 1.5 μm and infrared-to-visible upconversion emission, upon excitation at 976 nm, are evaluated as a function of the Er^{3+} concentration. For the lowest Er^{3+} content, 1.5 μm emission quantum efficiency was 90%. Increasing the Er^{3+} concentration up to 2 mol%, the emission quantum efficiency was observed to decrease to 37% due to concentration quenching. The green and red upconversion emission intensity ratio was studied as a function of Yb^{3+} co-doping and the Er^{3+}–Er^{3+} energy transfer processes.

II.1 Upconversion Spectroscopy

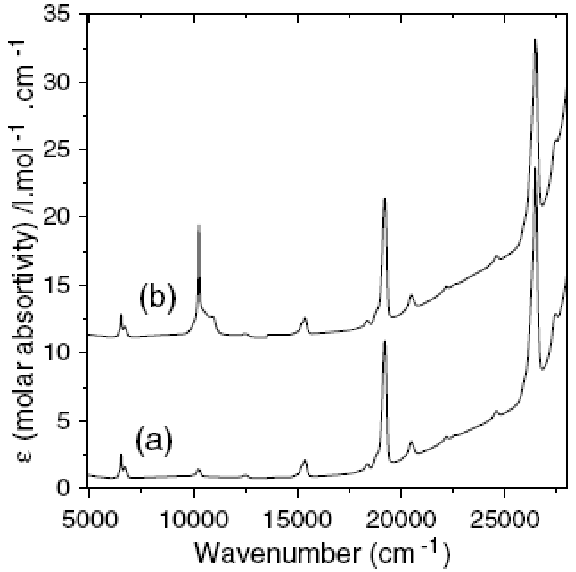

Fig. 1. Room temperature absorption spectra (a) 2.0 mol% Er^{3+} and (b) 2.0 mol% Yb^{3+} and 2.0 mol% Er^{3+}.

Table 1

Experimental (P_{EXP}) and calculated (P_{ED}) oscillator strengths obtained for the 2 mol% Er^{3+} glass sample, and Judd–Ofelt intensity parameters $\Omega_2 = 7.5 \times 10^{-20}$ cm^2, $\Omega_4 = 1.4 \times 10^{-20}$ cm^2 and $\Omega_6 = 0.7 \times 10^{-20}$ cm^2

Er^{3+} transition $^4I_{15/2} \rightarrow$	$\bar{\nu}$ (cm^{-1})	P_{EXP} (10^6)	P_{ED} (10^6)
$^4G_{11/2}$	26410	21.2	21.1
$^2H_{9/2}$	24570	0.49	0.47
$^4F_{5/2} + {}^4F_{3/2}$	22173	0.41	0.57
$^4F_{7/2}$	20490	1.37	1.38
$^2H_{11/2}$	19158	11.8	11.9
$^4S_{3/2}$	18381	0.28	0.30
$^4F_{9/2}$	15310	1.72	1.72
$^4I_{9/2}$	12499	0.29	0.33
$^4I_{11/2}$	10235	0.52	0.52
$^4I_{13/2}$	6553	1.03 (P_{MD} excluded)	0.90

The RMS of the fitting procedure was 9.3×10^{-8}.

II.1 Upconversion Spectroscopy

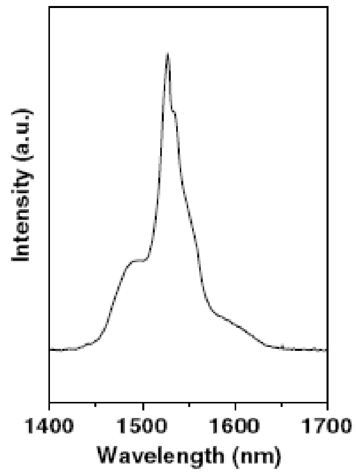

Fig. 2. Room temperature infrared emission spectrum for the 2.0 mol% Er^{3+} sample under 976 nm excitation.

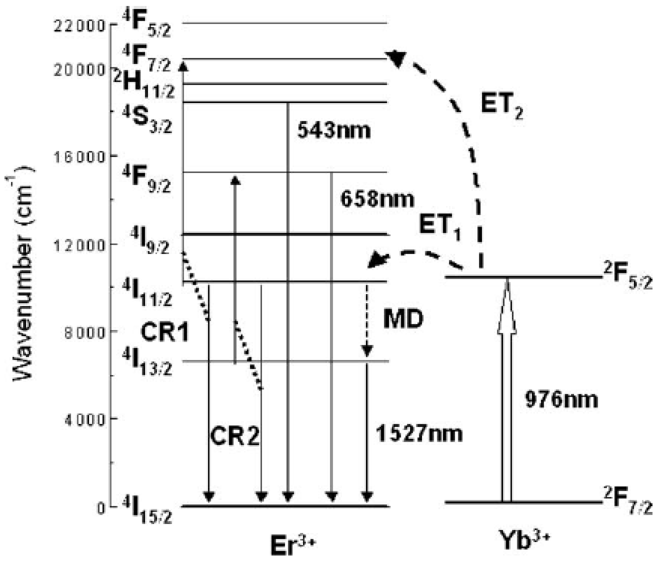

Fig. 3. Er^{3+} and Yb^{3+} free ion energy levels. The arrows indicate the excitation and relaxation processes discussed in the text.

II.1 Upconversion Spectroscopy

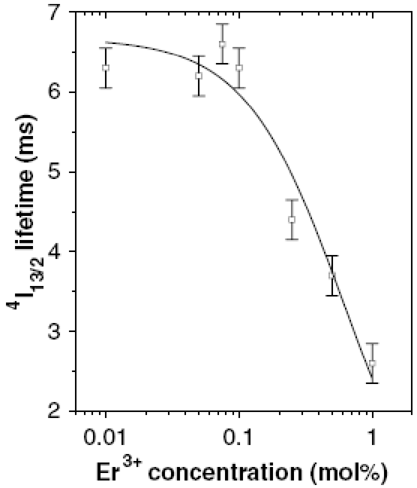

Fig. 5. Er^{3+} $^4I_{13/2}$ level lifetime values as a function of Er^{3+} concen
The line is just a guide for the reader.

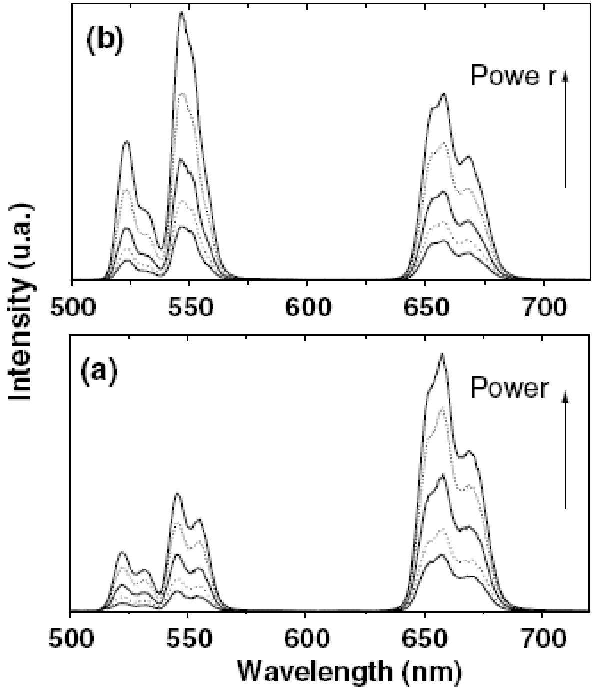

Fig. 6. Upconversion emission spectra as a function of the excitation power at 976 nm: (a) 2 mol% Yb^{3+} and 1.0 mol% Er^{3+} sample, (b) 2 mol% Yb^{3+} and 2.0 mol% Er^{3+} sample. The 976 nm pump power increase is indicated by the arrow for values of 100, 120, 150, 200, and 230 mW.

II.1 Upconversion Spectroscopy

COMMUNICATIONS

Blue upconversion enhancement by a factor of 200 in Tm^{3+}-doped tellurite glass by codoping with Nd^{3+} ions

N. Rakov, G. S. Maciel,[a] M. L. Sundheimer, L. de S. Menezes, and A. S. L. Gomes
Departamento de Física, Universidade Federal de Pernambuco, 50670-901 Recife-PE, Brazil

Y. Messaddeq, F. C. Cassanjes, G. Poirier, and S. J. L. Ribeiro
Instituto de Química, Universidade do Estado de São Paulo, P.O. Box 355, 14801-970 Araraquara-SP, Brazil

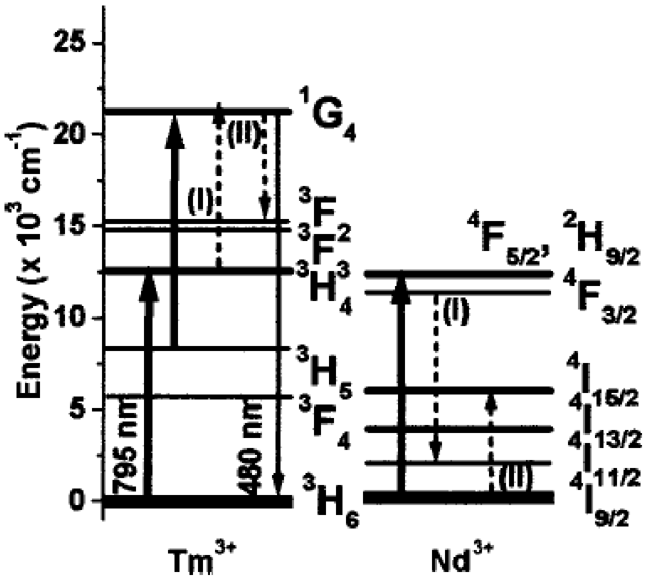

FIG. 3. Energy level schematic and the relevant channels responsible for the blue upconversion at 480 nm.

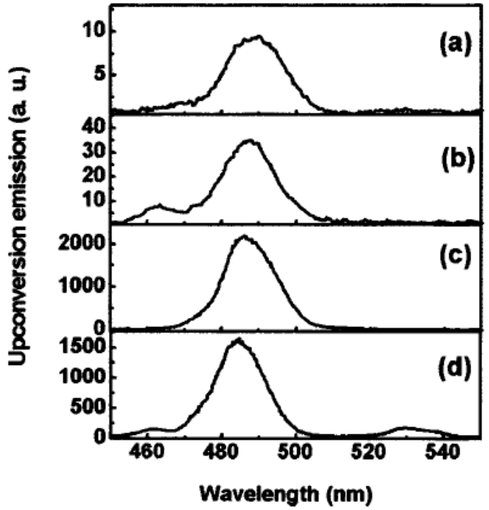

FIG. 1. Upconverted signal for (a) tellurite glass doped with Tm^{3+} (0.2 mol %); (b) ZBLAN glass doped with Tm^{3+} (0.2 mol %); (c) tellurite glass codoped with Tm^{3+} (0.2 mol %) and Nd^{3+} (0.5 mol %); (d) ZBLAN glass codoped with Tm^{3+} (0.2 mol %) and Nd^{3+} (0.5 mol %); upon near-infrared (795 nm) excitation.

II.1 Upconversion Spectroscopy

Cooperative absorption

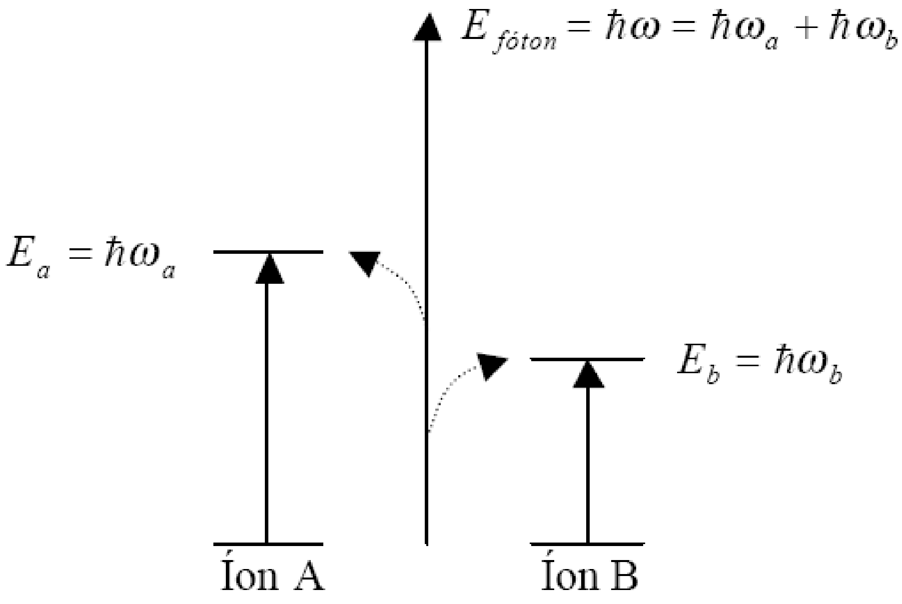

See more in Auzel's review article

Photon avalanche

II.1 Upconversion Spectroscopy

Case, W. E.; Koch, M. E.; Kueny, A. W. *J. Lumin*. **1990**, *45*, 351.

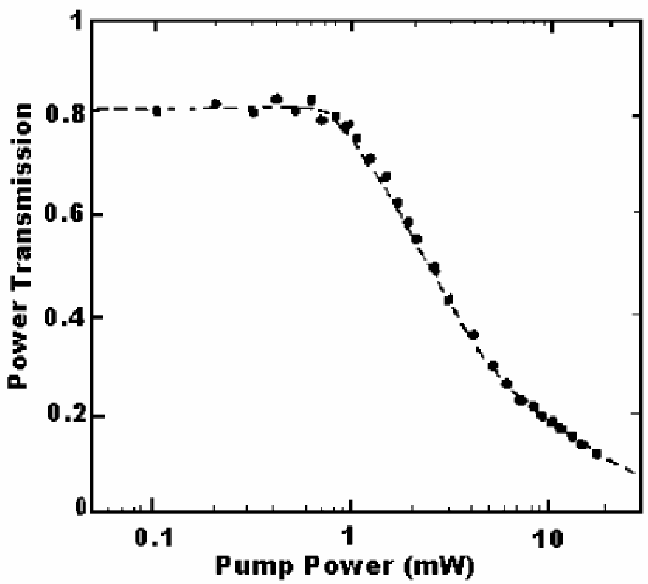

Figure 23. Decrease of transmission in a Pr^{3+}:$LaCl_3$ sample under $^3H_5$–$^3P_1$ pumping. (Reprinted with permission from ref 12. Copyright 1990 Elsevier.)

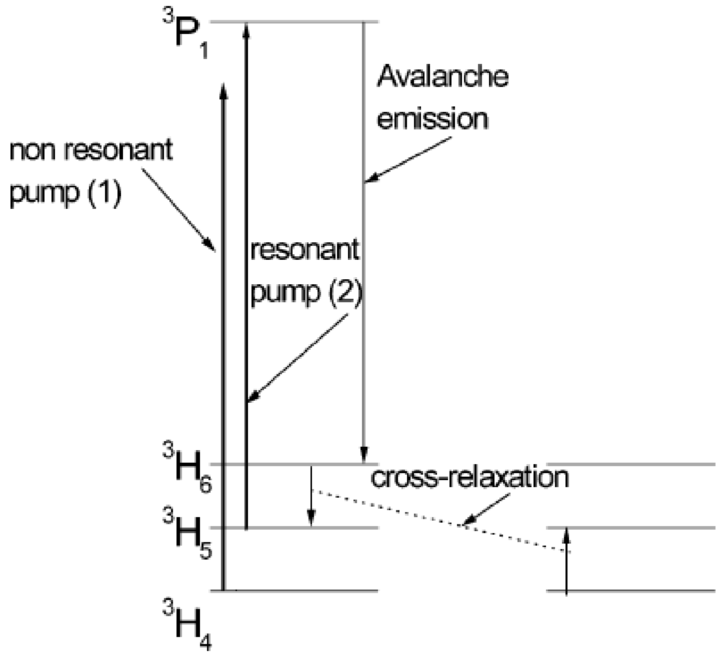

II.1 Upconversion Spectroscopy

Optics Communications
Volume 103, Issues 5-6 , 1 December 1993, Pages 361-364

Diode pumped avalanche upconversion in Pr^{3+}-doped fibers

A. S. L. Gomes, G. S. Maciel, R. E. de Araújo, L. H. Acioli and Cid B. de Araújo

Universidade Federal de Pernambuco, Departamento de Física, 50739, Recife, Brazil

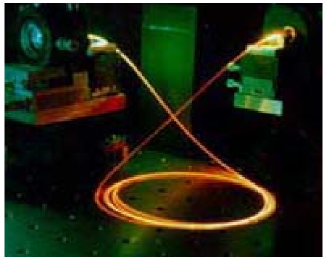

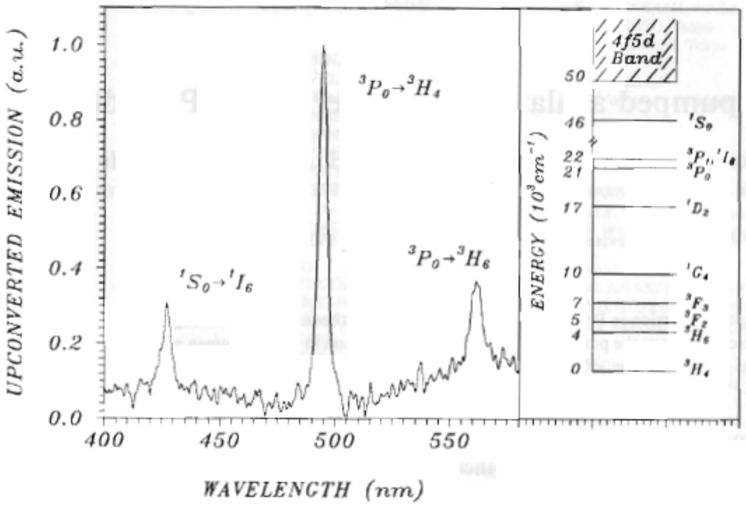

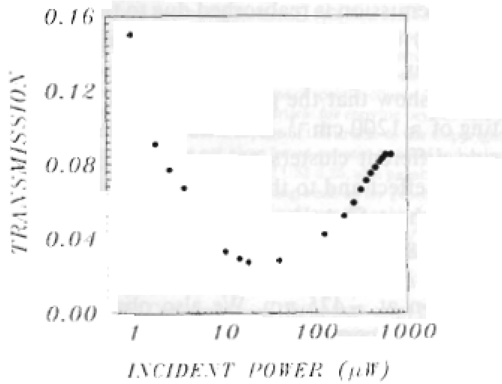

Fig. 2. Total beam transmission through a 3.5 m long SiO_2 based fiber doped with Pr^{3+} as a function of the laser incident power.

REDG Ceramics

Several products:

Cook-top panels
dinnerware
electronics
medicine
dentistry

- Tough materials
- Zero ou negative thermal expansion
- Can be made TRANSPARENT!

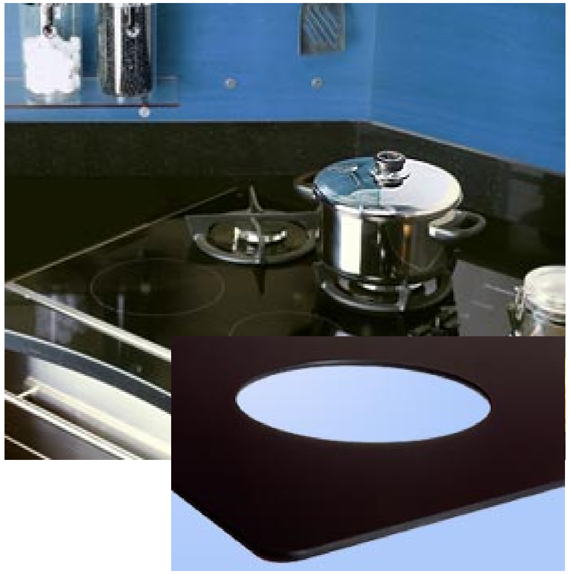

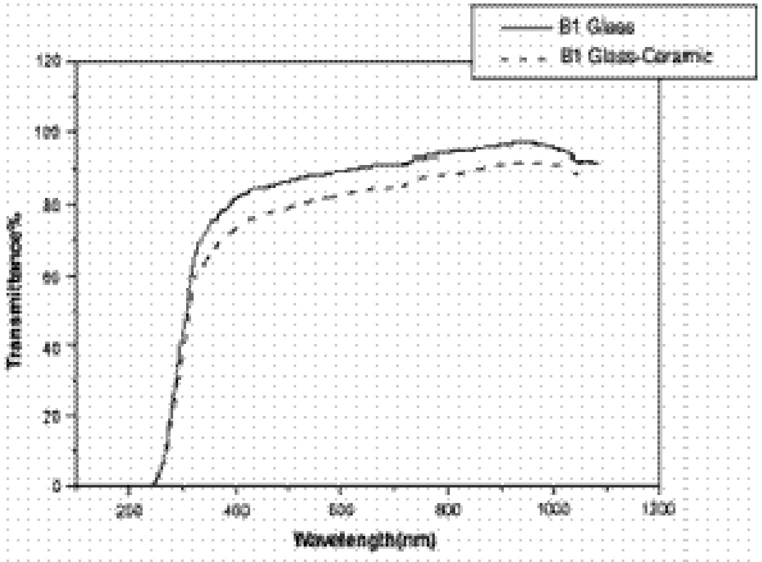

(a)

http://www.ch.seikei.ac.jp/kojima/Environmental/index%201.htm

II.2 REDG Ceramics

REDG Ceramics

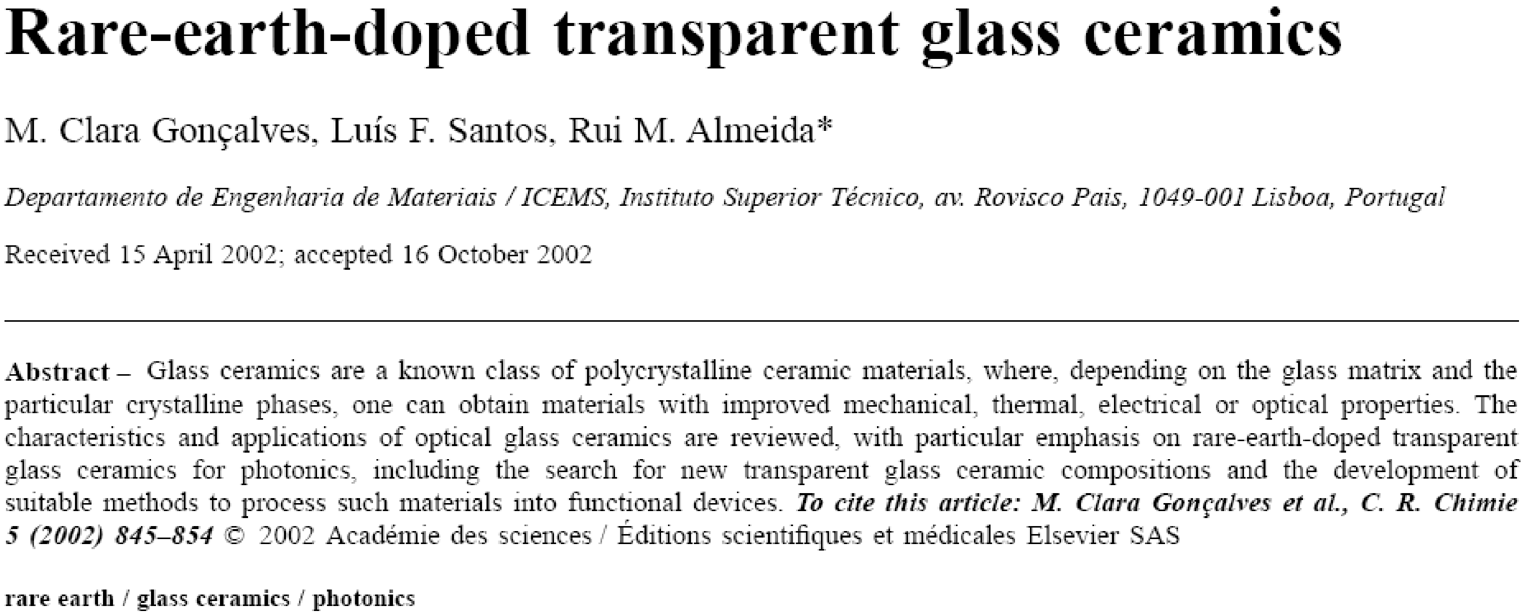

Rare-earth-doped transparent glass ceramics

M. Clara Gonçalves, Luís F. Santos, Rui M. Almeida*

Departamento de Engenharia de Materiais / ICEMS, Instituto Superior Técnico, av. Rovisco Pais, 1049-001 Lisboa, Portugal

Received 15 April 2002; accepted 16 October 2002

Abstract – Glass ceramics are a known class of polycrystalline ceramic materials, where, depending on the glass matrix and the particular crystalline phases, one can obtain materials with improved mechanical, thermal, electrical or optical properties. The characteristics and applications of optical glass ceramics are reviewed, with particular emphasis on rare-earth-doped transparent glass ceramics for photonics, including the search for new transparent glass ceramic compositions and the development of suitable methods to process such materials into functional devices. ***To cite this article: M. Clara Gonçalves et al., C. R. Chimie 5 (2002) 845–854*** © 2002 Académie des sciences / Éditions scientifiques et médicales Elsevier SAS

rare earth / glass ceramics / photonics

Rare Earth doped transparent glass-ceramics

M. Mortier, M. Génotelle, G. Patriarche

http://www.solgel.com/articles/Dec00/glass/envitromm.html

REDG Ceramics

•Crystal sizes well below incident light wavelength present negligible attenuation due to scattering! (Rayleigh-Gans theory).

•Requires a refractive index difference <0.1 between amorphous and crystalline phases.

Driving applications:

large telescope mirror blanks
liquid crystal displays
solar cells
photonic devices (lasers, amplifiers, upconverters, etc)

II.2 REDG Ceramics

Rare Earth doped transparent glass-ceramics

M. Mortier, M. Génotelle, G. Patriarche

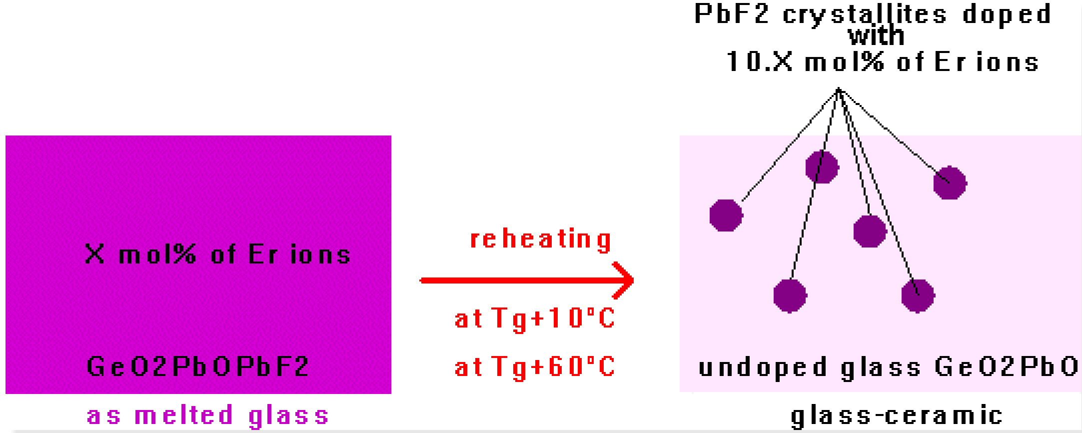

Germanate oxyfluorides glass of the family :

$(50GeO_2 50\text{-}y PbO\, y PbF_2 + x ErF_3)$

y, y=[10,20] x=[0,4]

Rare Earth doped transparent glass-ceramics

M. Mortier, M. Génotelle, G. Patriarche

II.2 REDG Ceramics

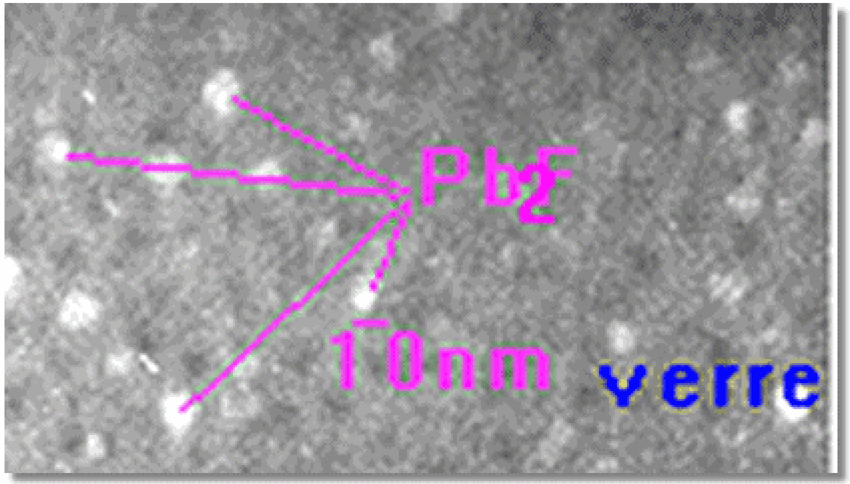

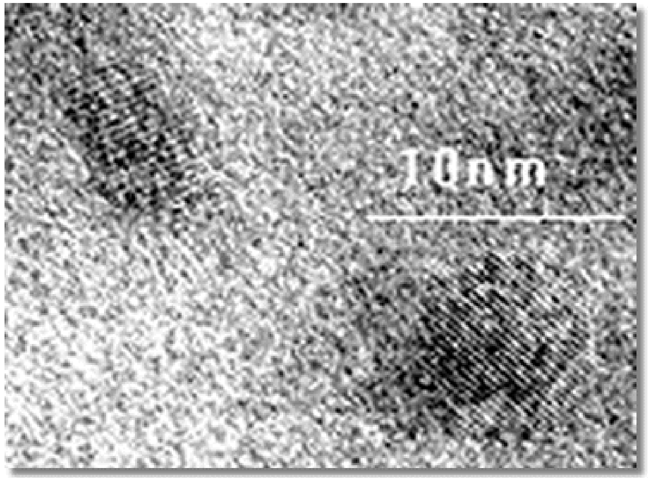

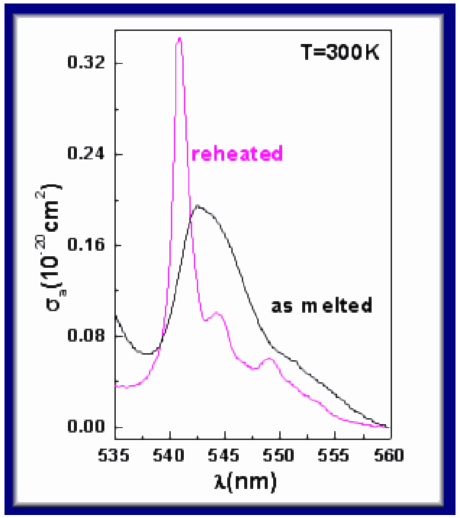

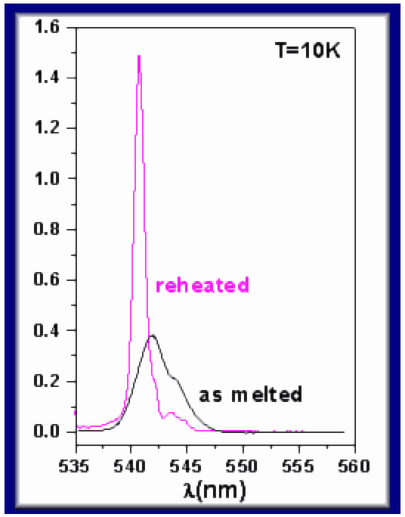

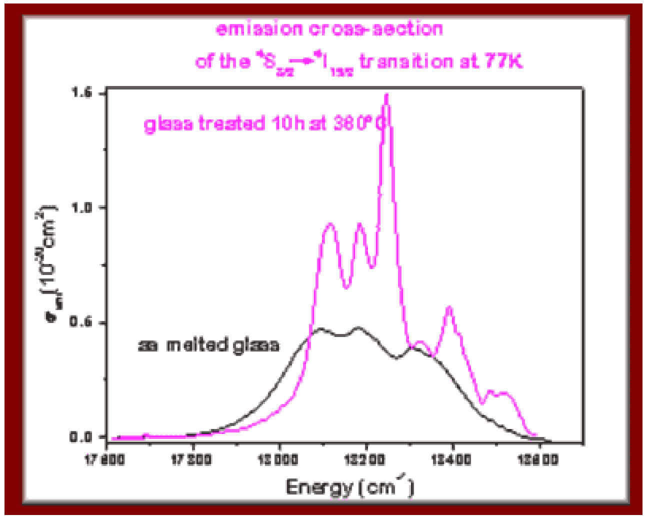

II.2 REDG Ceramics

M. Clara Gonçalves et al. / C. R. Chimie 5 (2002) 845–854

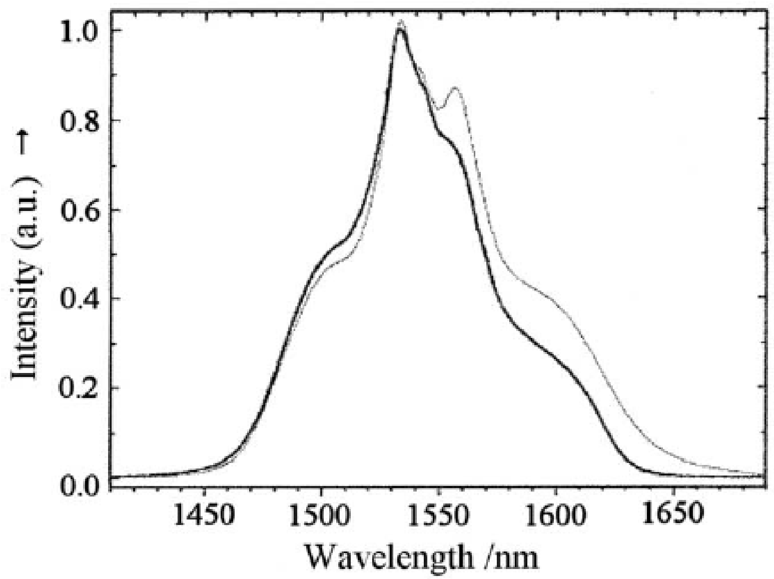

Fig. 2. Normalised photoluminescence spectra of Er^{3+} ($^4I_{13/2} \rightarrow {}^4I_{15/2}$ transition) in the precursor oxyfluoride glass (thick solid line) and in a developed glass ceramic heat treated at 440 °C for 5 h (dashed line). (Adapted from ref. [38].)

Other glass ceramics:

Silicate oxyfluoride
Tellurite oxyhallides
and more (see M C G review).

Applications of REDG

II.3 REDG for Lasers
II.4 REDG for Fiber Lasers and
Amplifiers
II.5 REDG Planar and Channel
Waveguides
II.6 REDG Microbarcodes

II.3 REDG for LASERS

REDG for Lasers

Nd:YAG (crystal), Nd:Glass

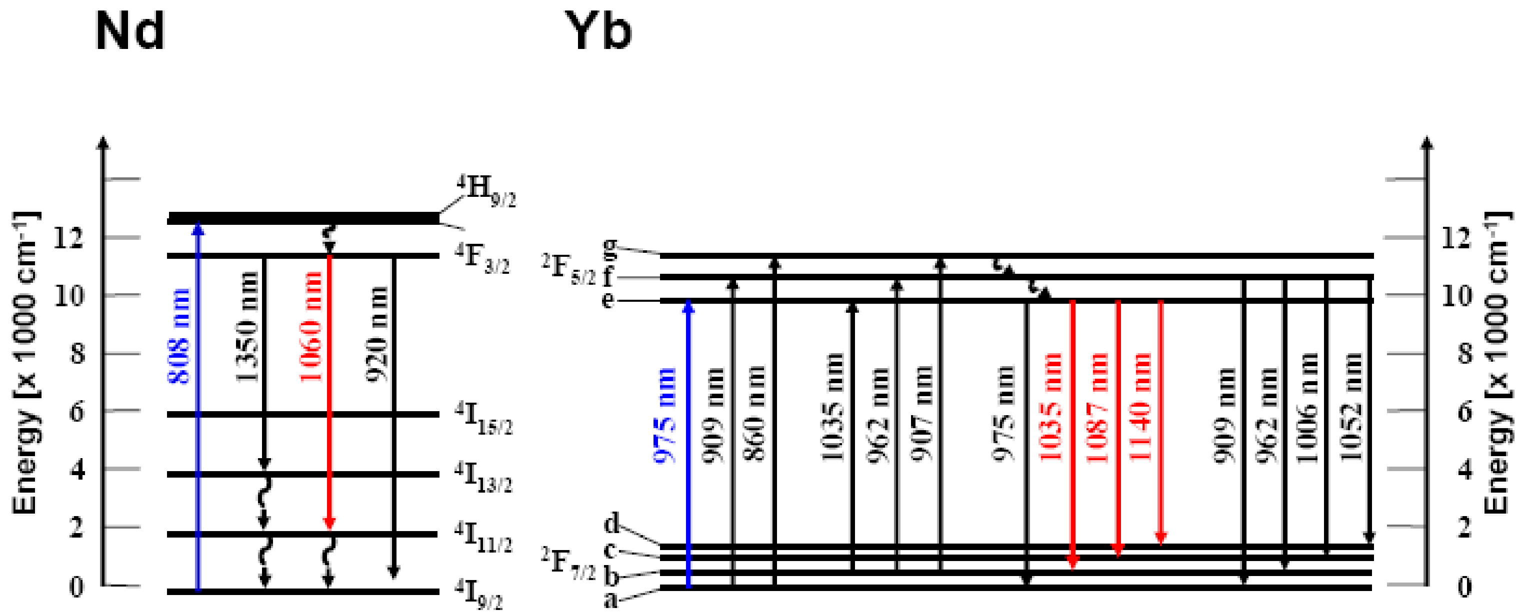

II.3 REDG for LASERS

Typical pump geometries

end pumped laser rod

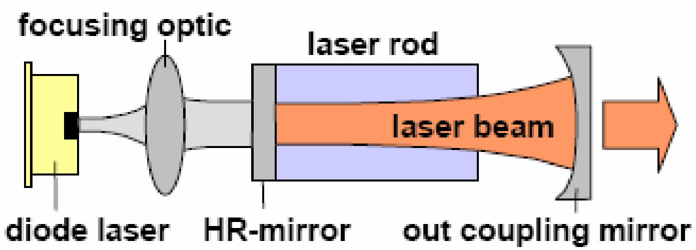

side pumped laser rod

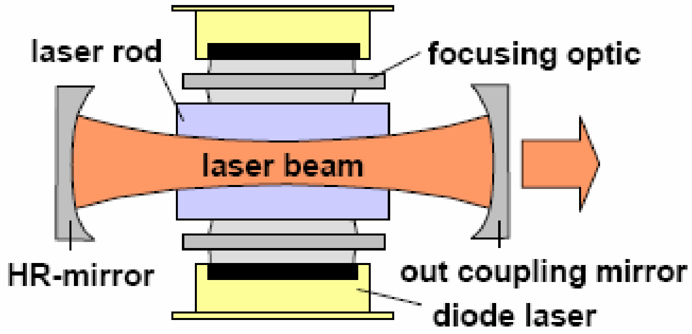

Fraunhofer Institut Angewandte Optik und Feinmechanik

Institute of Applied Physics

Niche application

II.3 REDG for LASERS

Electronic Control System for Table-Top Terawatt Nd:Glass Laser

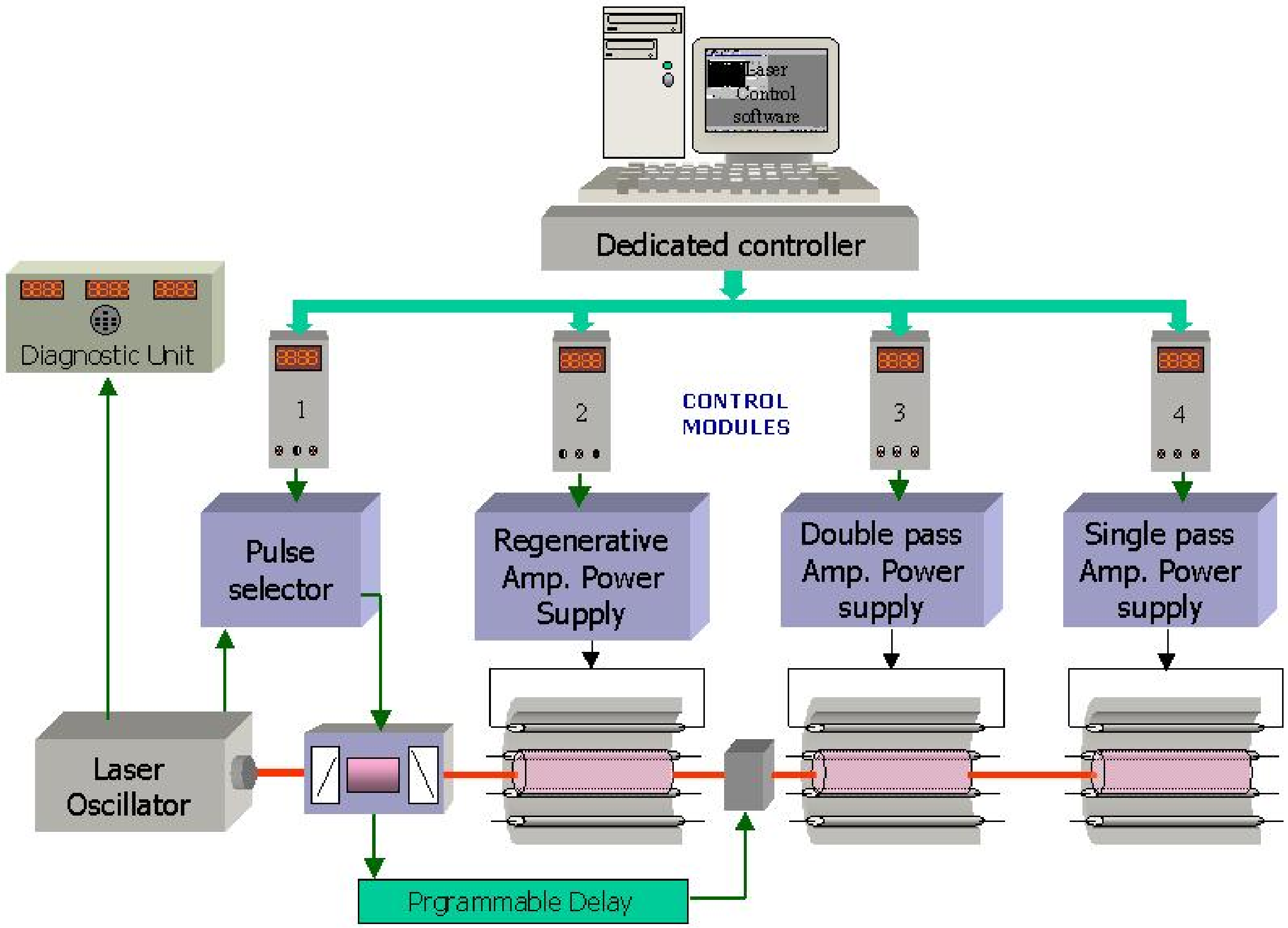

REDG for Fiber Lasers and Amplifiers

II.3 REDG for Fiber Lasers and amplifiers

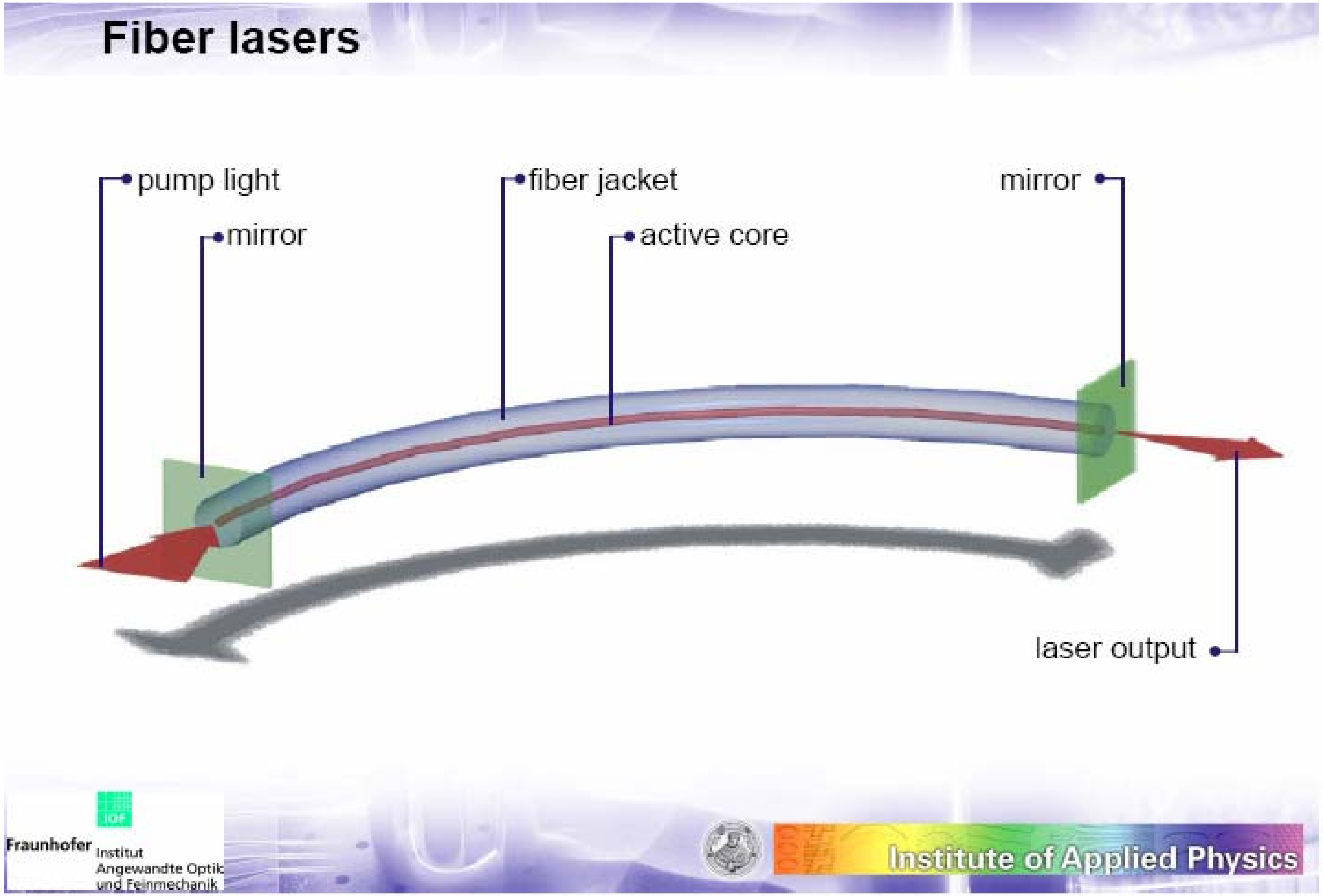

REDG for Fiber Lasers and Amplifiers

II.3 REDG for Fiber Lasers and amplifiers

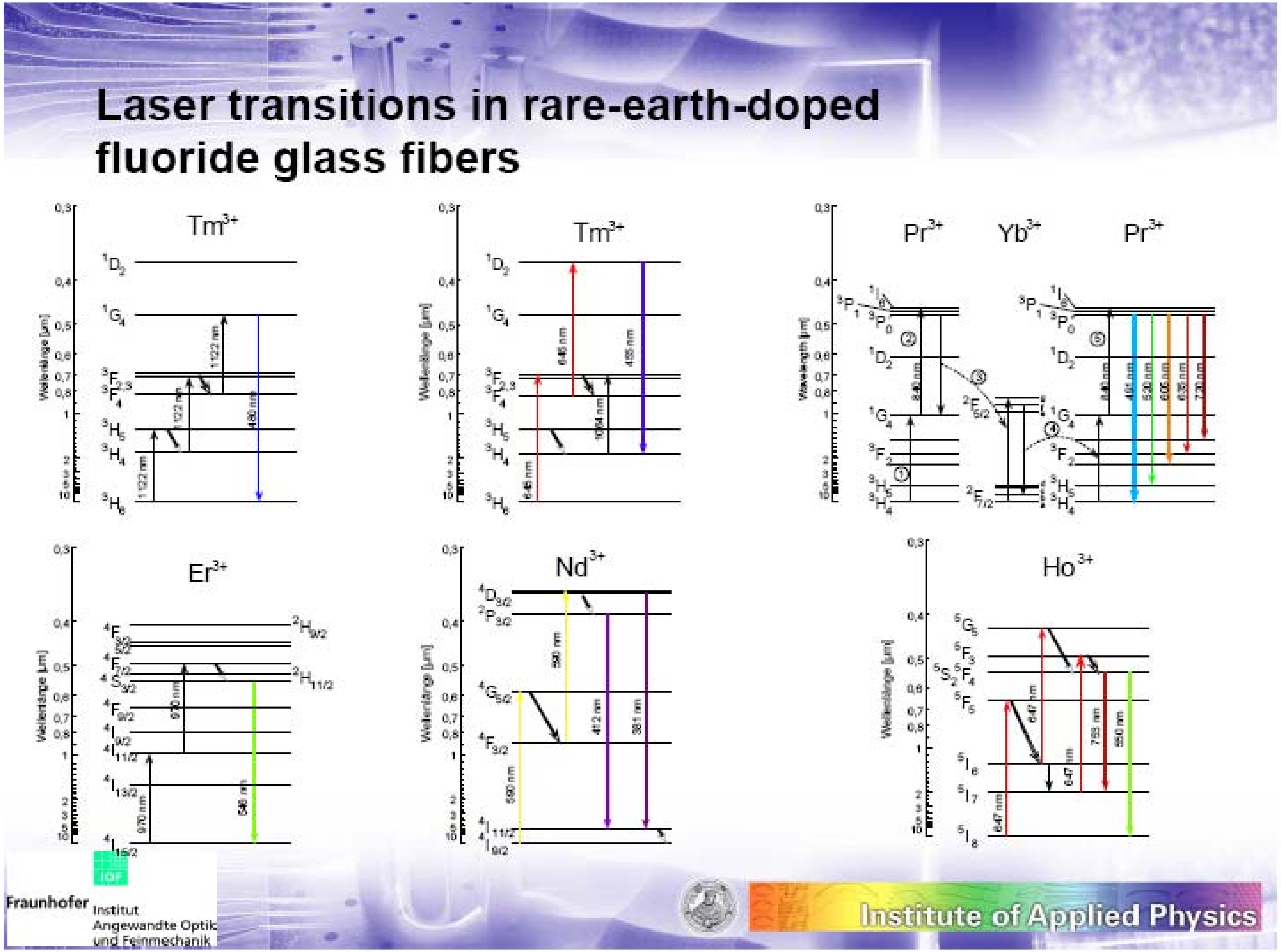

II.3 REDG for Fiber Lasers and amplifiers

Fiber Laser: emission wavelength

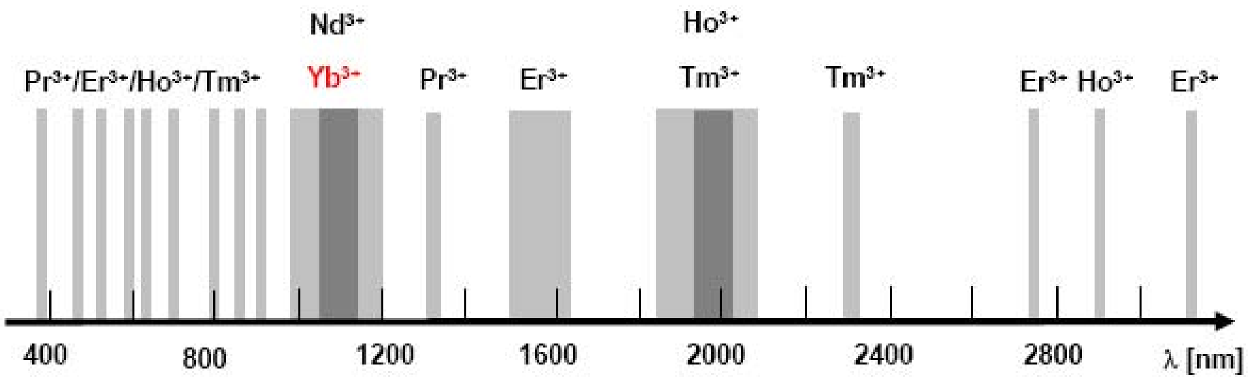

first demonstration of a fiber laser: in the early sixties !

E. Snitzer, "Neodymium glass laser," Proc. of the Third International conference on Solid Lasers, Paris, page 999 (1963).
C.J. Koester and E.Snitzer, "Amplification in a fiber laser," Appl. Opt. 3, 10, 1182 (1964).

Er: upconversion fiber laser

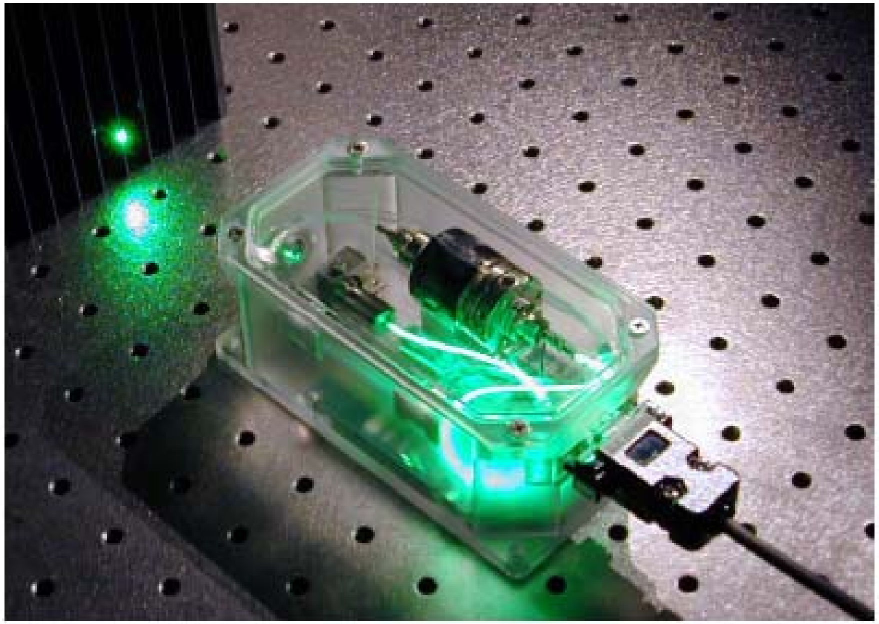

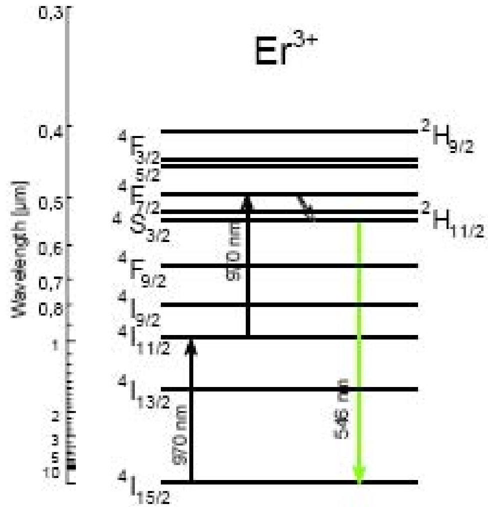

Thulium doped upconversion fiber laser

II.3 REDG for Fiber Lasers and amplifiers

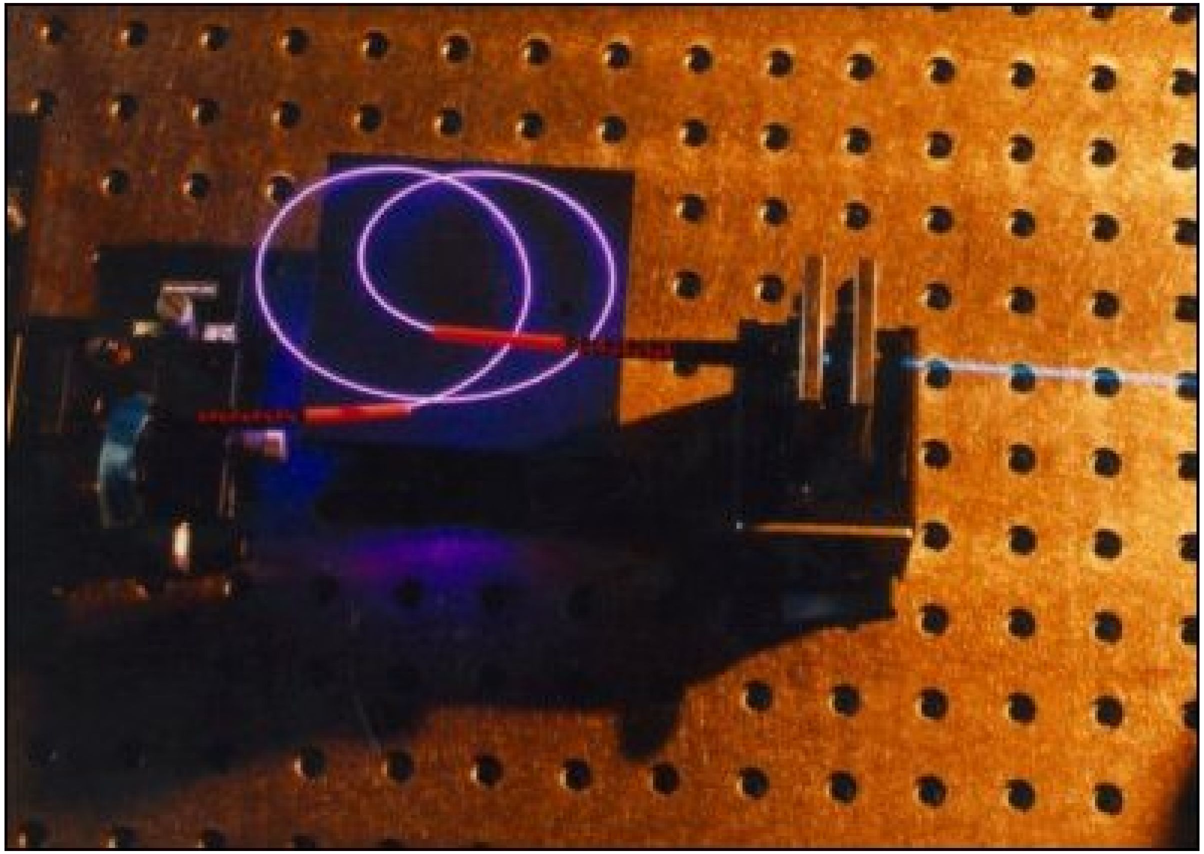

Fiber Amplifiers

II.3 REDG for Fiber Lasers and amplifiers

C. R. Chimie 5 (2002) 815–824

S1631074802014492/REV

REVUE / ACCOUNT

Rare-earth-doped glasses for fiber amplifiers in broadband telecommunication

Setsuhisa Tanabe*

Faculty of Integrated Studies, Kyoto University, Kyoto 606-8501, Japan

Received 30 April 2002; accepted 28 May 2002

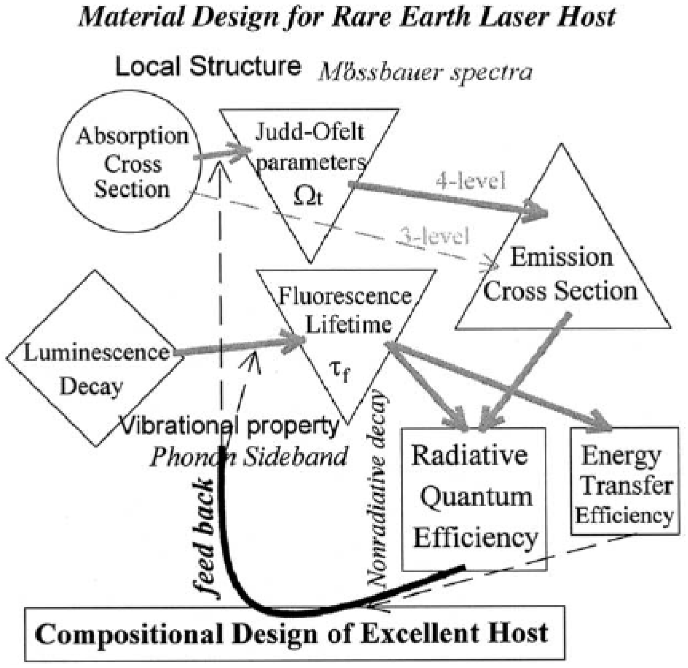

Fig. 2. Research scheme for efficient laser materials.

Optical Amplifiers Diversity

II.3 REDG for Fiber Lasers and amplifiers

REDFA, such as:

PDFA

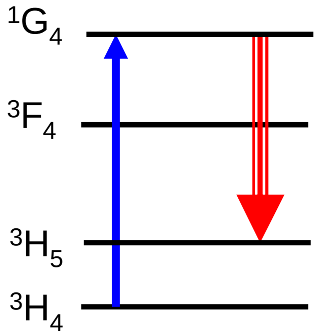

EDFA

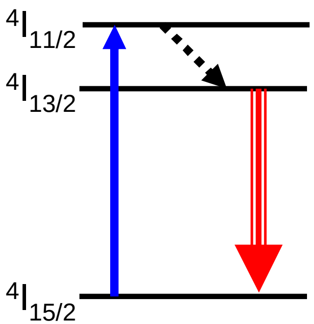

TDFA

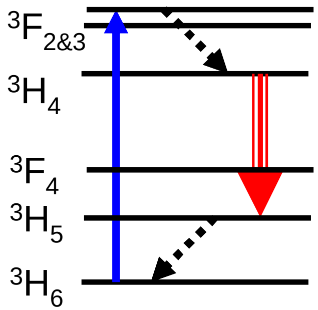

HYBRIDS

parallel

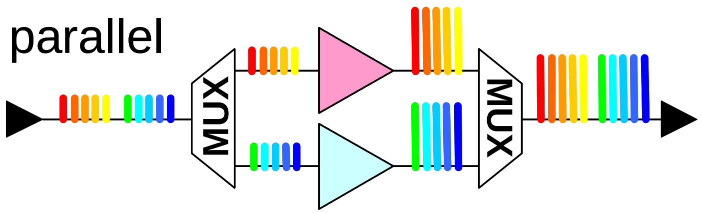

series

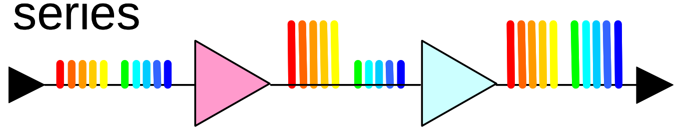

Importance of the host glass

II.3 REDG for Fiber Lasers and amplifiers

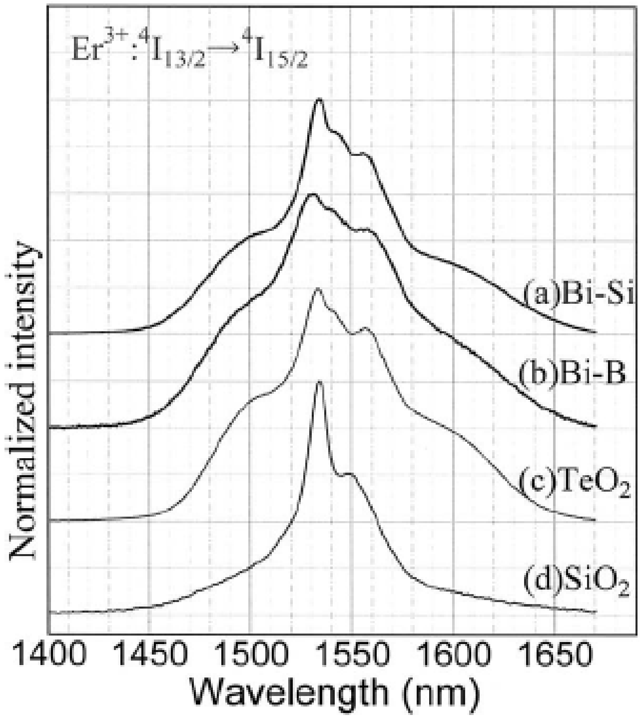

Fig. 3. Fluorescence spectra of Er^{3+}-doped glasses; (a) Bi-silicate, (b) Bi-borate, (c) Tellurite and (d) Al-silica.

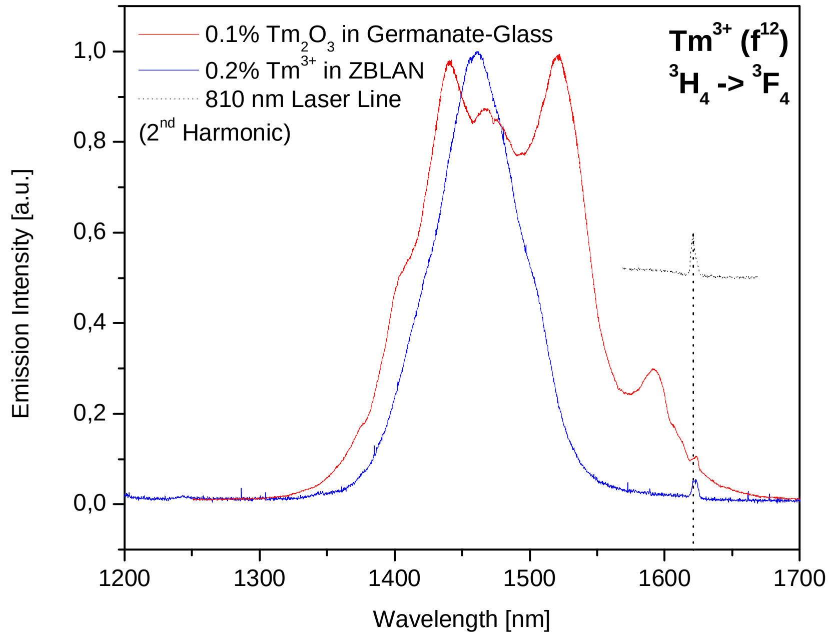

II.3 REDG for Fiber Lasers and amplifiers

Importance of understanding REE
S-band (1450nm-1510nm) TDFA

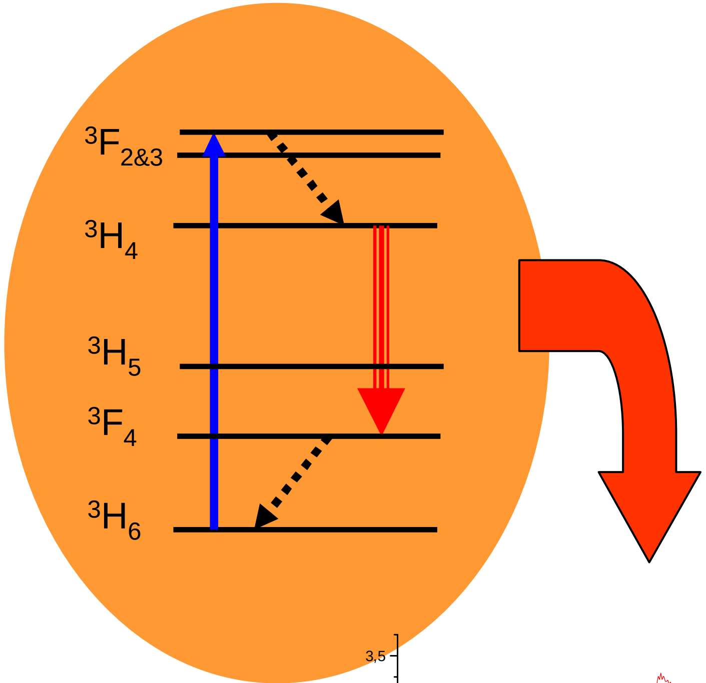

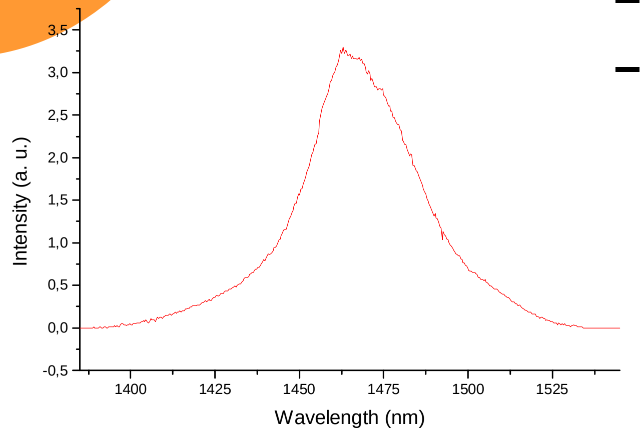

+ S-band emission: $^3H_4 \rightarrow {}^3F_4$

+ Conversion efficiency
+ Low loss in non-operation
+ Diode pump sources

– Multi-phonon relaxation
– Material reliability
– Lifetime bottleneck
– Complex pump schemes

TDFA – Pumping Schemes

Single wavelength pump

II.3 REDG for Fiber Lasers and amplifiers

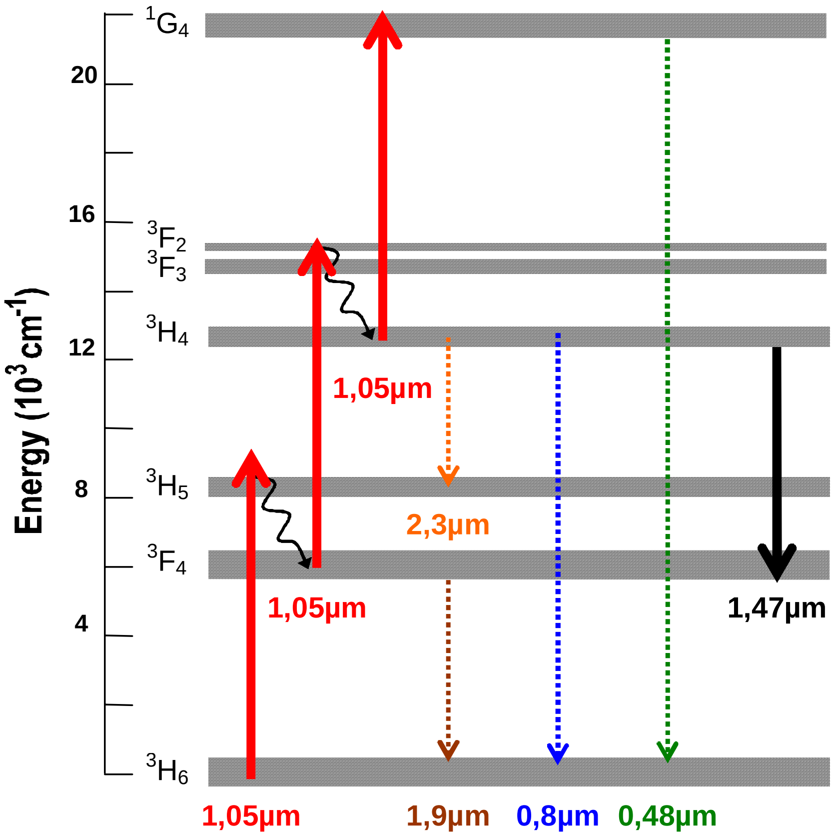

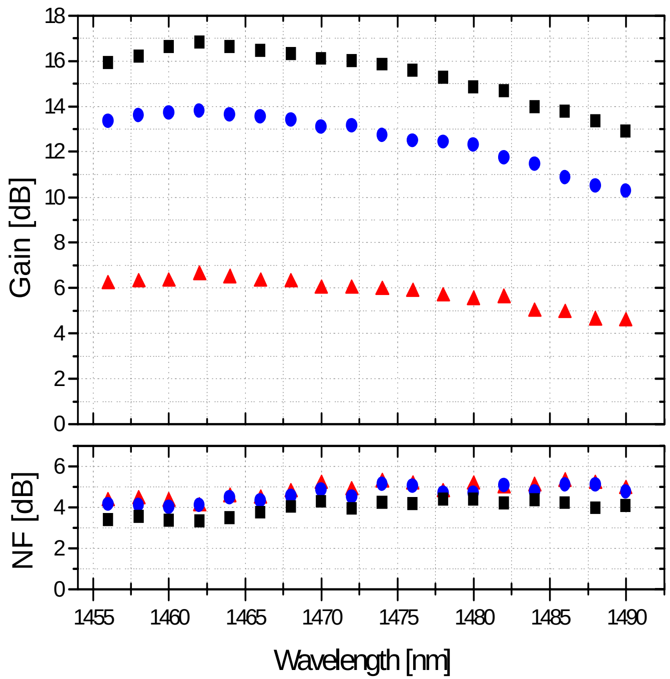

Gain and NF as function of the signal wavelength. The pump powers are: ■ 400mW, ● 300mW and ▲ 150mW.

•Komukai and co-workers, IEEE J.Quant. Electr. 31, 1880 (1995).

•Aozasa and co-workers, Elect. Lett. 37, 1157 (2001).

II.3 REDG for Fiber Lasers and amplifiers

Dual-wavelength pump schemes (preferred, more efficient)

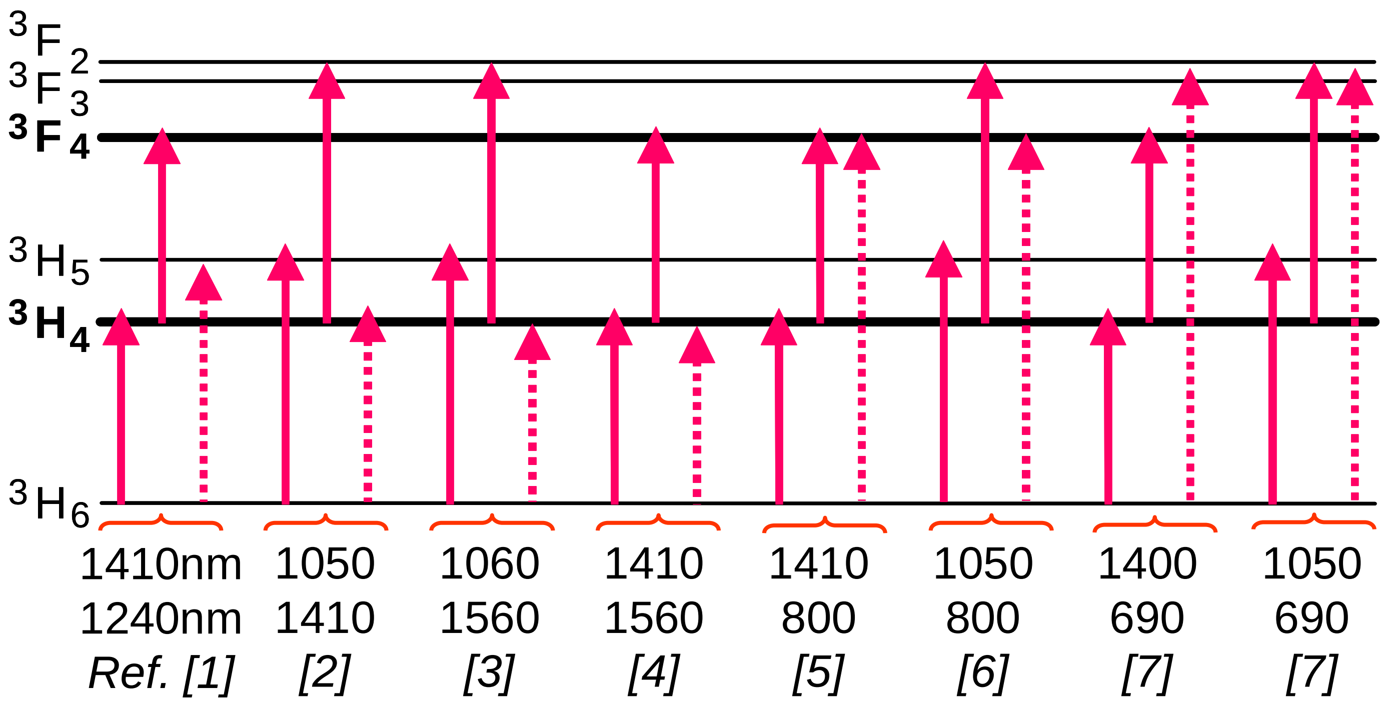

References

[1] F. Roy, Electron.Lett. **37**, *2001*, 943
[2] B. Cole, Proc.OFC 2001, paper TuQ3
[3] T. Kasamatsu, Opt.Lett. **24**, *1999*, 1684
[4] T. Kasamatsu, Photon.Technol. Lett. **13**, *2001*, 433
[5] F. Roy, OSA TOP,**60**, *2001*, 24
[6] A.S.L. Gomes, Opt.Lett. **28**, *2003*, 334
[7] S.S-H. Yam, Proc. OFC 2005, paper OWF4

800nm+1050nm Pump Scheme for TDFA

II.3 REDG for Fiber Lasers and amplifiers

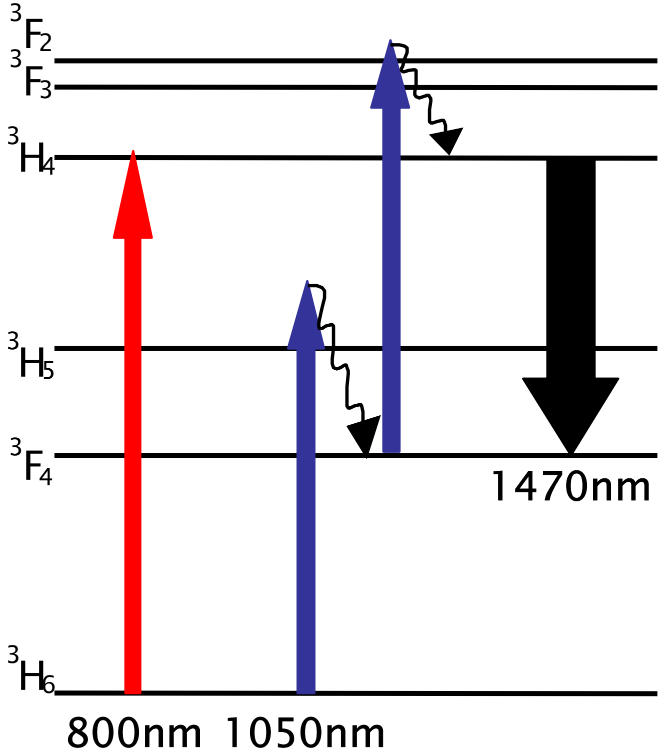

800nm

GSA – Populates directly the higher amplifying level

1050nm

ESA – Depopulates the lower level + populate the higher level

FB2 9:15am POST-DEADLINE OFC 2002

Novel dual wavelength (1050 nm + 800 nm) pumping scheme for thulium doped fiber amplifiers

A.S.L.Gomes, M.L. Sundheimer, M.T. Carvalho, J.F. Martins-Filho, C.J.A. Bastos-Filho, Univ. Federal de Pernambuco, Brazil; W. Margulis, ACREO, Sweden.

Contact e-mail: anderson@df.ufpe.br

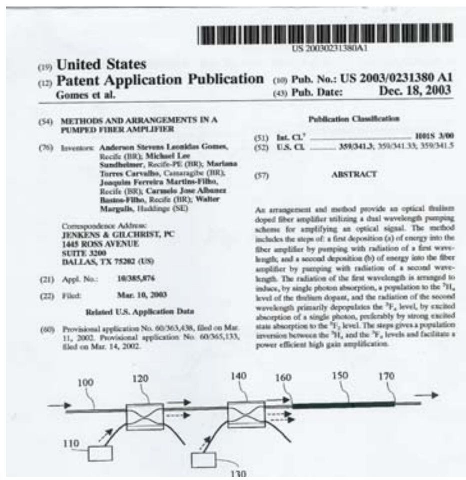

US 20030231380A1

(19) United States
(12) Patent Application Publication (10) Pub. No.: US 2003/0231380 A1
Gomes et al. (43) Pub. Date: Dec. 18, 2003

(54) METHODS AND ARRANGEMENTS IN A PUMPED FIBER AMPLIFIER

(76) Inventors: Anderson Stevens Leonidas Gomes, Recife (BR); Michael Lee Sundheimer, Recife-PE (BR); Mariana Torres Carvalho, Camaragibe (BR); Joaquim Ferreira Martins-Filho, Recife (BR); Carmelo Jose Albanez Bastos-Filho, Recife (BR); Walter Margulis, Huddinge (SE)

Correspondence Address:
JENKENS & GILCHRIST, PC
1445 ROSS AVENUE
SUITE 3200
DALLAS, TX 75202 (US)

(21) Appl. No.: 10/385,876

(22) Filed: Mar. 10, 2003

Related U.S. Application Data

(60) Provisional application No. 60/363,438, filed on Mar. 11, 2002. Provisional application No. 60/365,133, filed on Mar. 14, 2002.

Publication Classification

(51) Int. Cl.^{7} H01S 3/00
(52) U.S. Cl. 359/341.3; 359/341.33; 359/341.5

(57) ABSTRACT

An arrangement and method provide an optical thulium doped fiber amplifier utilizing a dual wavelength pumping scheme for amplifying an optical signal. The method includes the steps of: a first deposition (a) of energy into the fiber amplifier by pumping with radiation of a first wavelength; and a second deposition (b) of energy into the fiber amplifier by pumping with radiation of a second wavelength. The radiation of the first wavelength is arranged to induce, by single photon absorption, a population to the $^3H_4$ level of the thulium dopant, and the radiation of the second wavelength primarily depopulates the $^3F_4$ level, by excited absorption of a single photon, preferably by strong excited state absorption to the $^3F_2$ level. The steps gives a population inversion between the $^3H_4$ and the $^3F_4$ levels and facilitate a power efficient high gain amplification.

100 120 140 160 150 170 110 130

Results for the 800+1050nm pumping scheme

II.3 REDG for Fiber Lasers and amplifiers

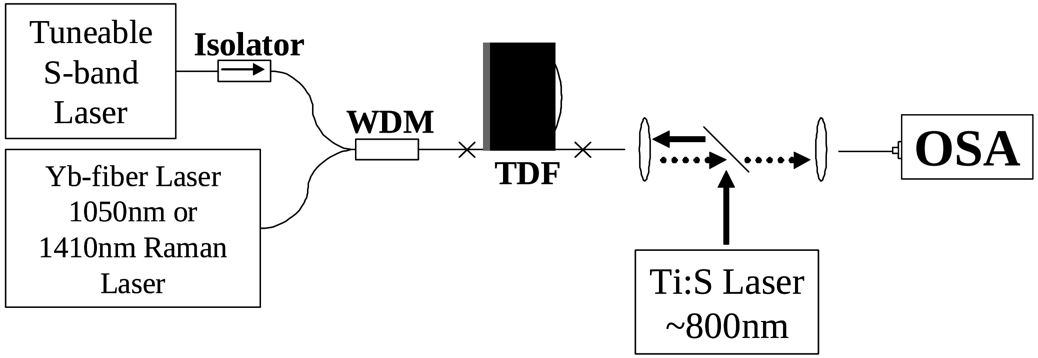

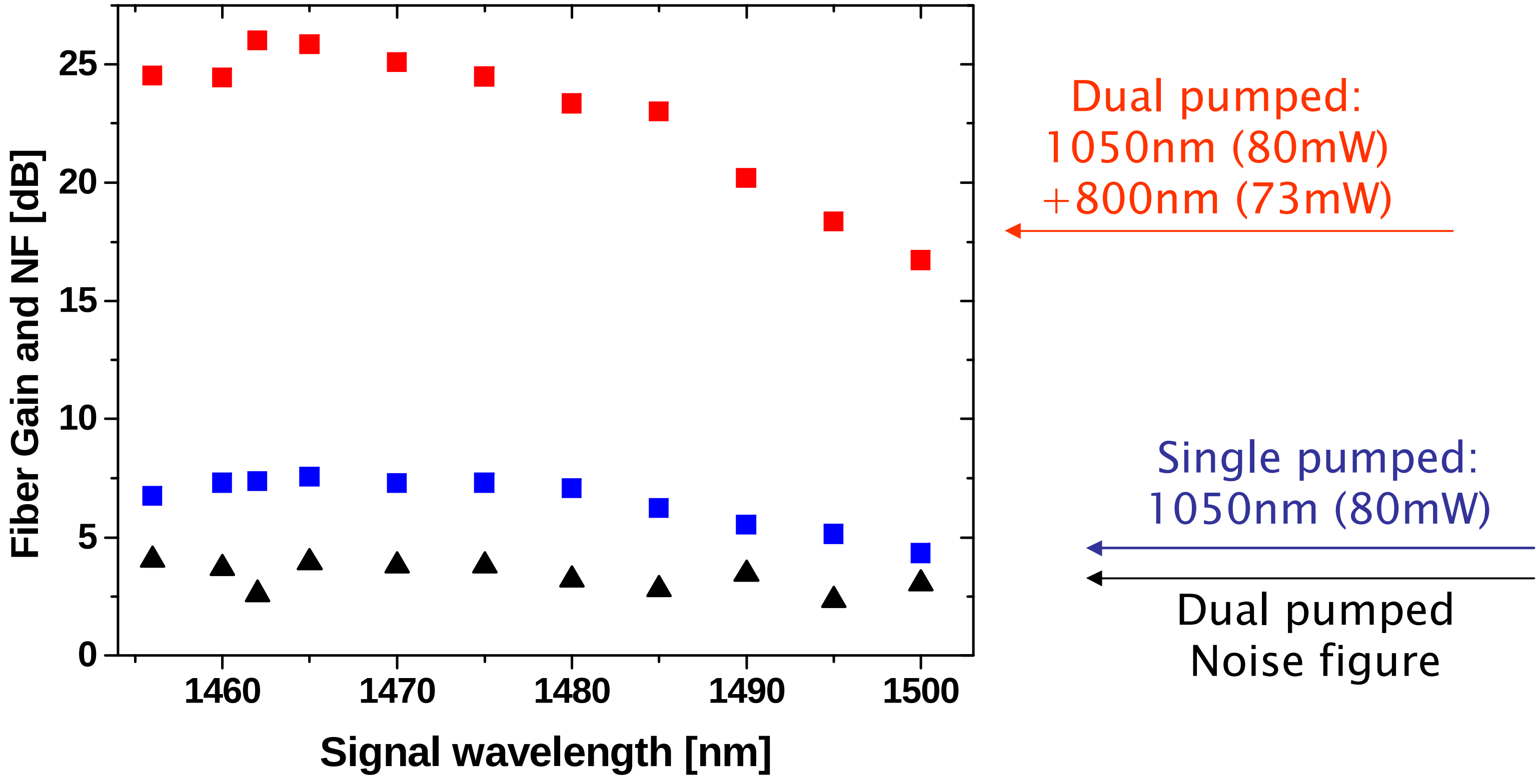

L = 18m, 2000ppm ZBLAN, Ps= -27dBm

Fiber Amplifiers

II.3 REDG for Fiber Lasers and amplifiers

Chirped-pulse-amplification

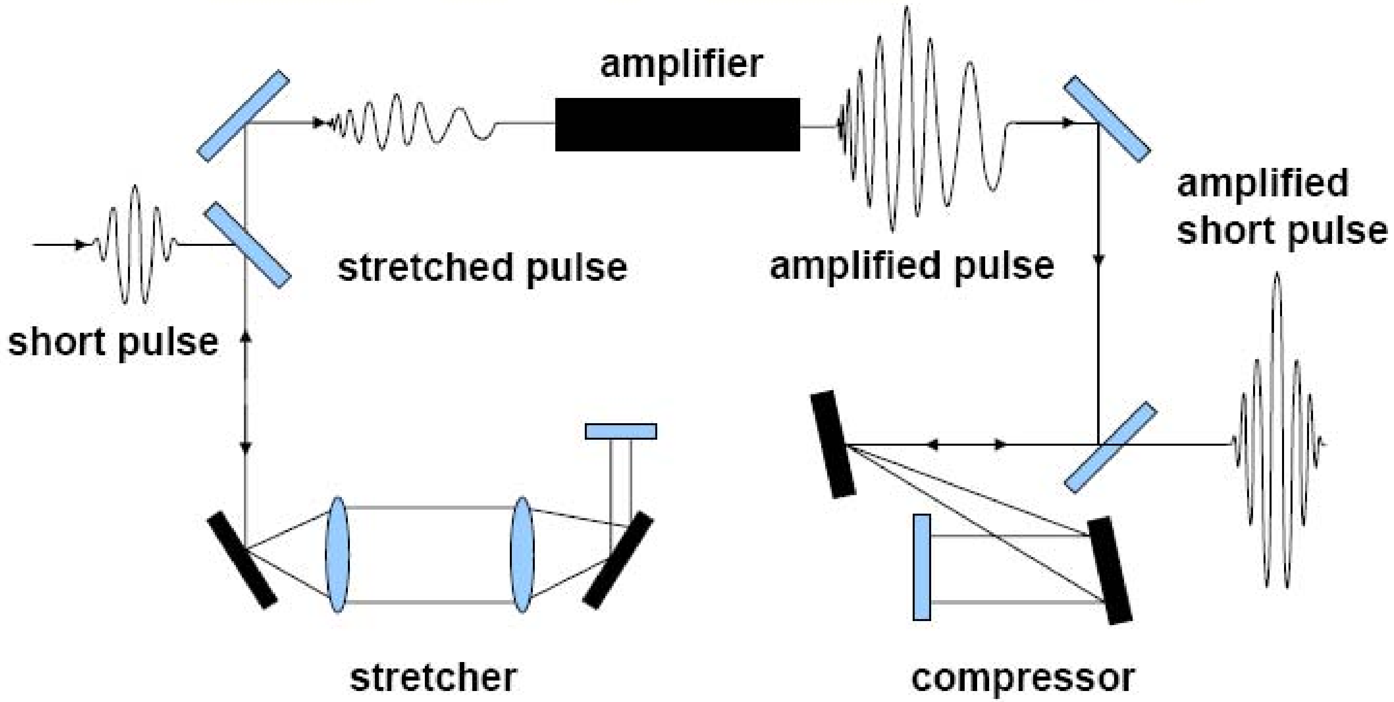

D. Strickland and G. Mourou, "Compression of amplified optical pulses," Opt. Comm. 56, 3, 219 (1985).

Fiber Amplifiers

II.3 REDG for Fiber Lasers and amplifiers

CPA-fiber amplifier – power amplifier

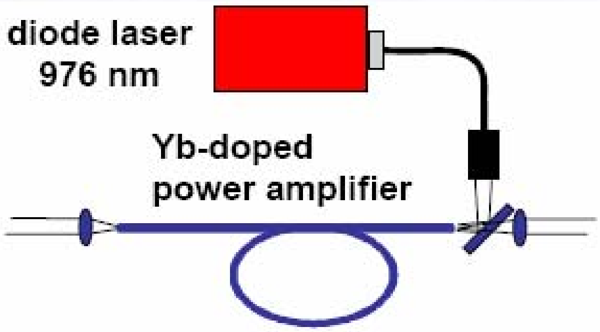

Yb-doped large-mode-area fiber

length: 13.5 m
core: ∅ = 28.5 µm, NA = 0.06, MFD = 23 µm
inner clad.: ∅ = 400 µm, NA = 0.38, D
doping: 700 ppm (mol) Yb_2O_3

beam quality:
diffraction-limited (M^2 = 1.1)

degree of polarization:
~ 50% (3 to 1)

output characteristics

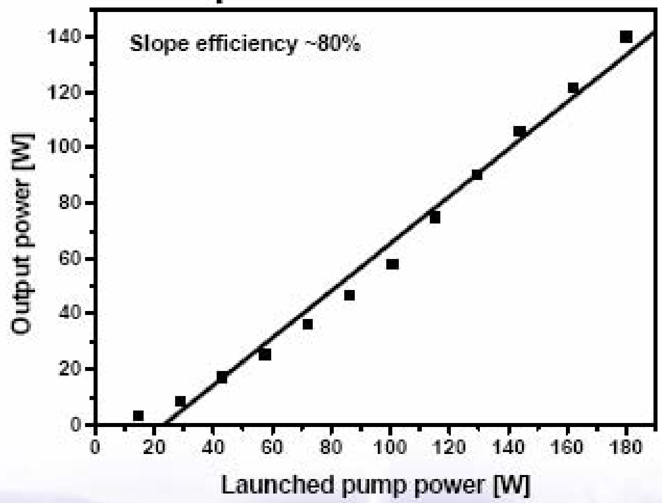

Fiber Amplifiers

II.3 REDG for Fiber Lasers and amplifiers

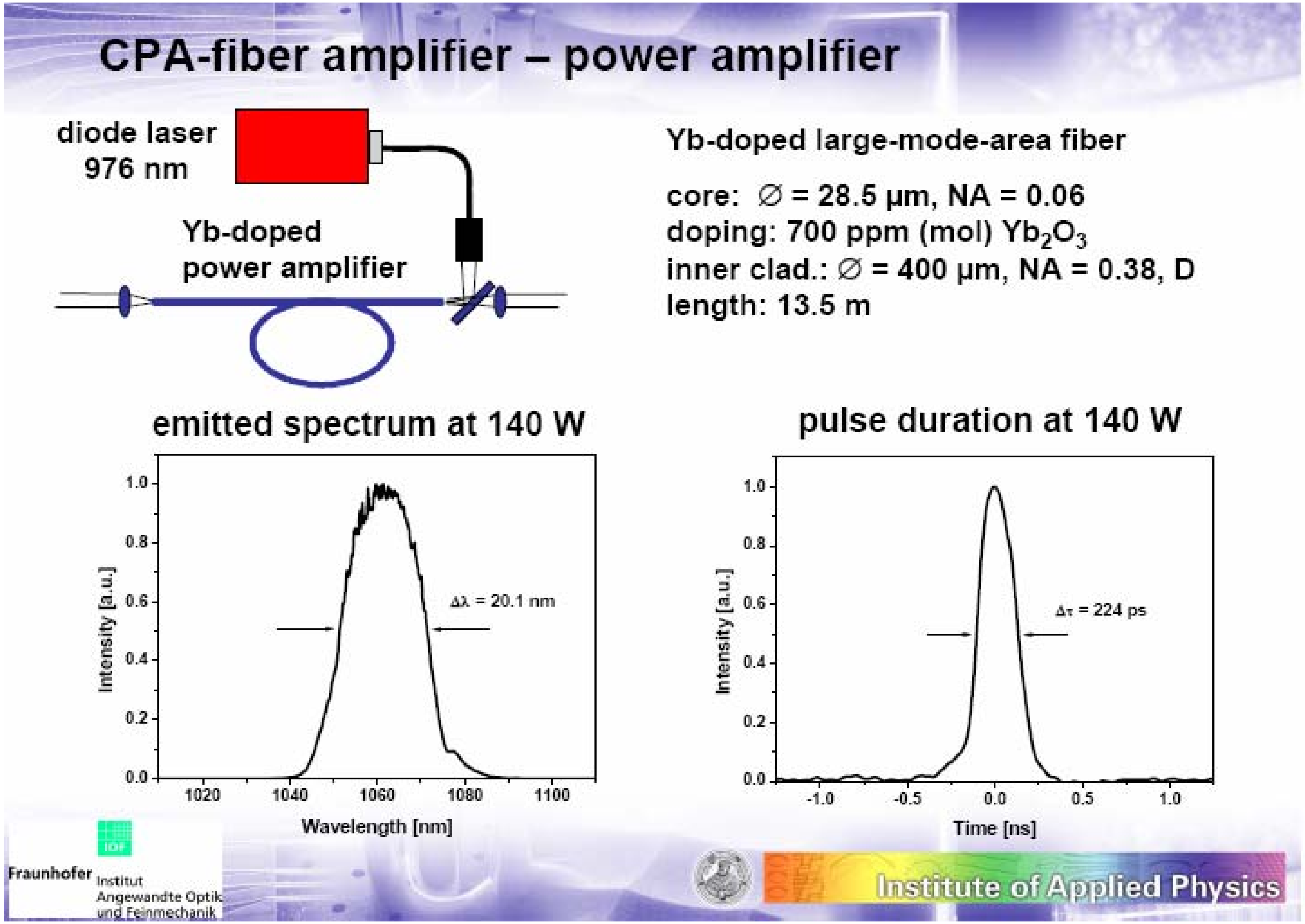

Fiber Amplifiers

II.3 REDG for Fiber Lasers and amplifiers

CPA-fiber amplifier – compressor stage

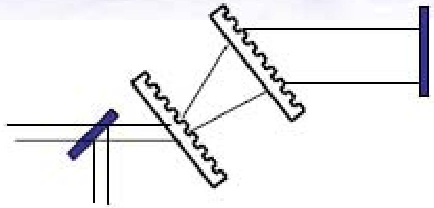

Output

transmission gratings in fused silica fabricated by electron beam lithography

grating separation: 61 cm
diffraction angle: 44.5° (3° off Littrow)

compressor efficiency

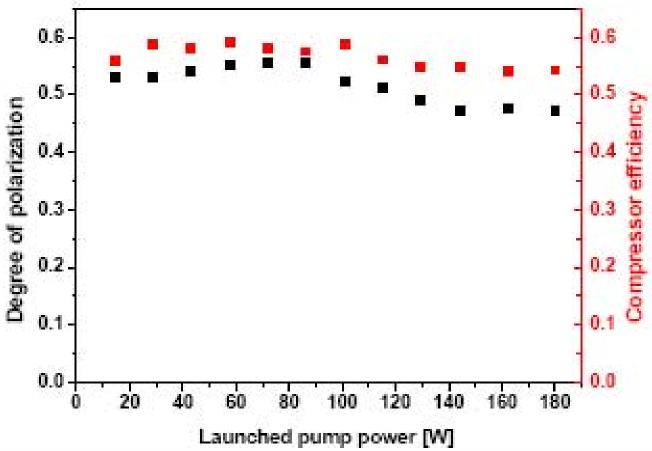

autocorrelation trace

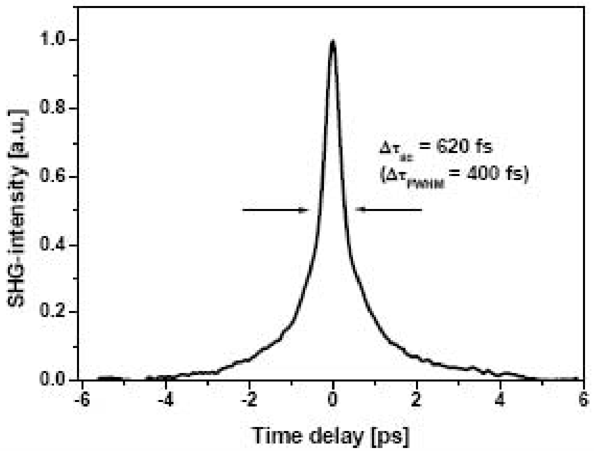

80 W average power of 400 fs pulses

Fraunhofer Institut Angewandte Optik und Feinmechanik

Institute of Applied Physics

REDG Planar and Channel Waveguides

II.4 REDG planar and channel waveguides

PLANAR WAVEGUIDE FABRICATION FACILITIES
DEPARTAMENTO DE FÍSICA - UFPE

Clean Room (class 1000)
(mask alignment, photolithography, etc)

Preparation methods employed:

- **Proton exchange and Ti-indifusion for $LiNbO_3$**
- **Ion Exchange for silicate glasses**
- **Nonmetalic indifusion for fluoroindate glasses**

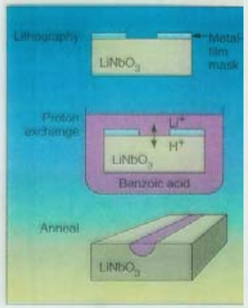

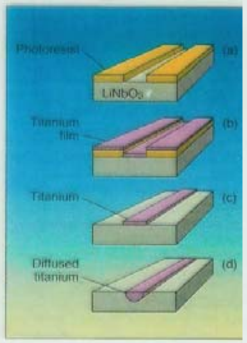

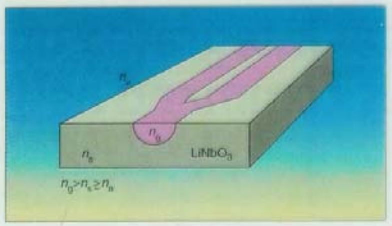

Characterization & Applications

LINEAR (losses, modes, Δn, etc)

NONLINEAR (e-o modulators, all-optical switches, lasers, amplifiers, etc)

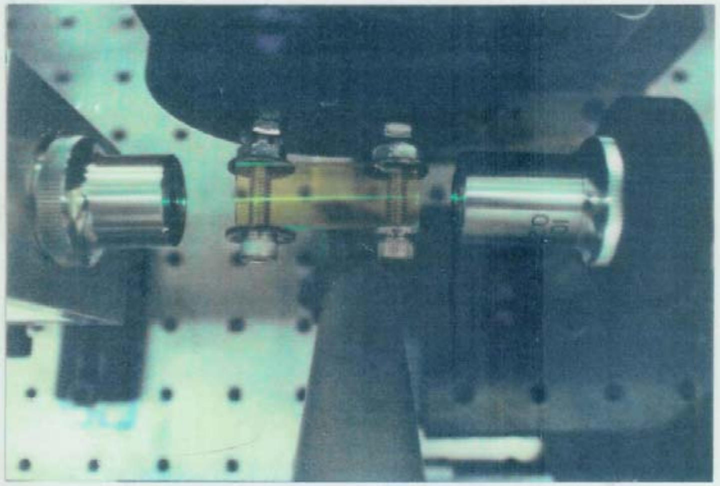

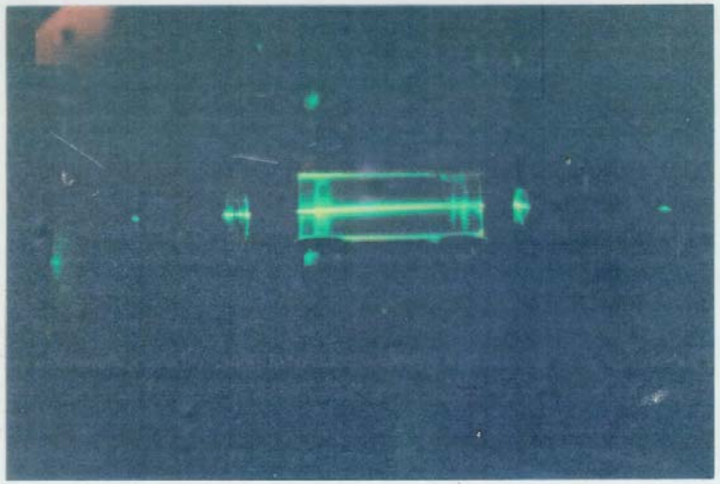

End Fire Coupling Into Waveguides

II.4 REDG planar and channel waveguides

All-optical switching in rare-earth doped channel waveguide

Cid B. de Araújo and A. S. L. Gomes
Departamento de Física, Universidade Federal de Pernambuco, 50670-901 Recife, PE, Brazil

R. Srivastava
Photonics Research Laboratory, University of Florida, Gainesville, Florida 32611

(Received 26 August 1994; accepted for publication 11 November 1994)

The operation of an all-optical switch in a rare-earth doped channel waveguide is described. The switching mechanism is based on an optically induced intramodal energy exchange, driven by a resonantly enhanced nonlinearity of a Nd^{3+} ion. Switching times around 410 μs at a repetition rate of 1 kHz was demonstrated. © *1995 American Institute of Physics.*

Appl. Phys. Lett. **66** (4), 23 January 1995

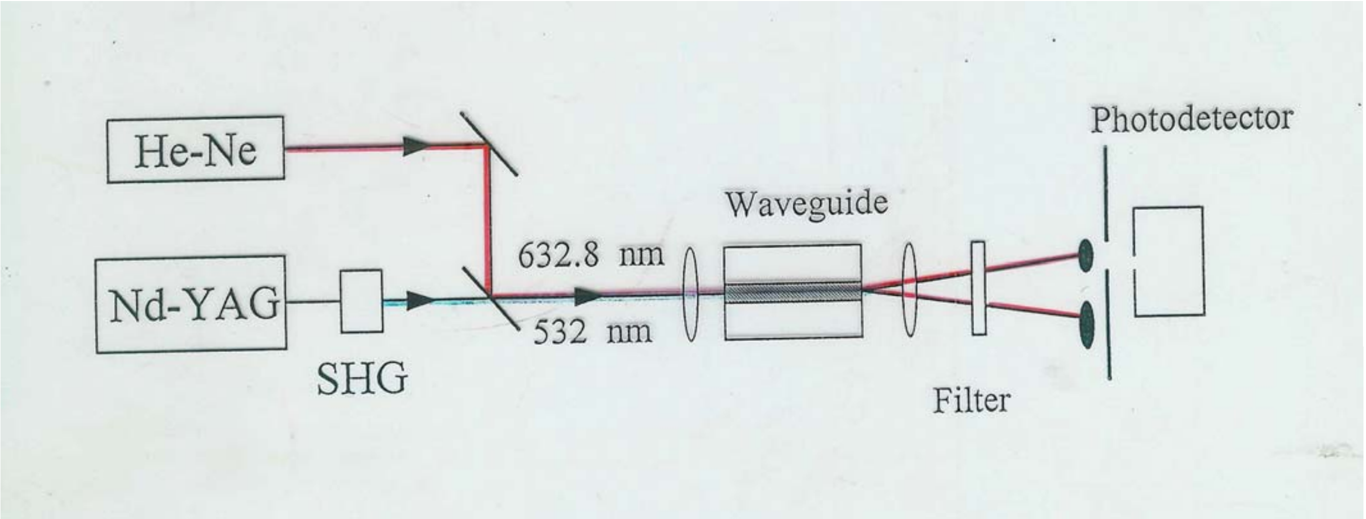

Ion exchange, 8mm long, 2-10μm width, $\Delta n = 8.7\times10^{-3}$

Silicate glass, 16%Na_2O, 2%Nd_2O_3, $K^+ \leftrightarrow Na^+$

II.4 REDG planar and channel waveguides

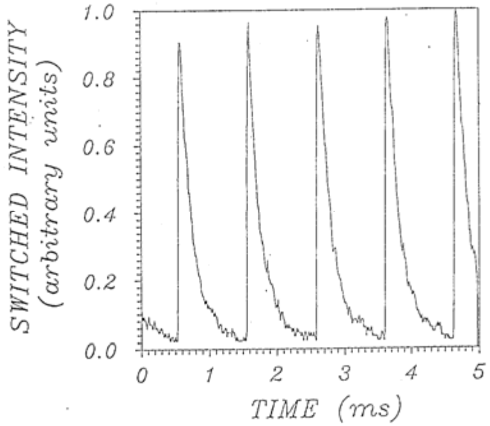

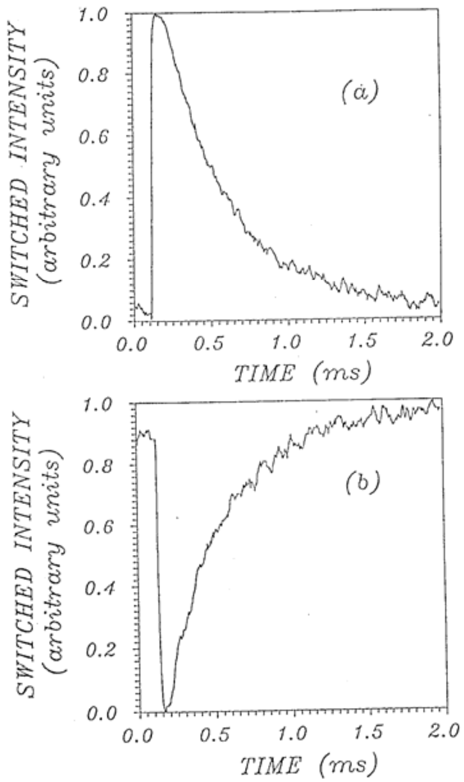

PHYSICAL MECHANISM FOR ALL-OPTICAL SWITCHING IN Nd-DOPED WAVEGUIDE

Energy exchange between two-lobes of a high order propagating mode.

First observed in RED optical fibres (Pantell et al. OL 92; Sadowski et al. OL 93). Fibre lengths of ~1m were employed.

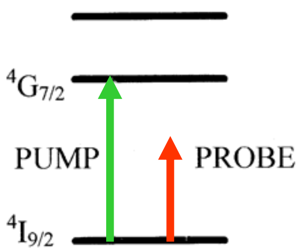

The pump beam resonantly induces a differential phase shift in the two spatial components of the signal beam.

As a consequence, a change in intensity occurs from one lobe to the other.

MAIN FEATURES:

The nature of the optical nonlinearity is electronic in origin.

Repetition rate limited by pump level lifetime (410μs).

Pump Power dependence: Linear

Estimated n_2 ~10^{-13}cm^2/W

II.4 REDG planar and channel waveguides

Fabrication and Characterization of Photonic Devices Directly Written in Glass Using Femtosecond Laser Pulses

Catalin Florea, *Member, IEEE, Member, OSA,* and Kim A. Winick, *Senior Member, IEEE, Member, OSA*

- writing geometry:

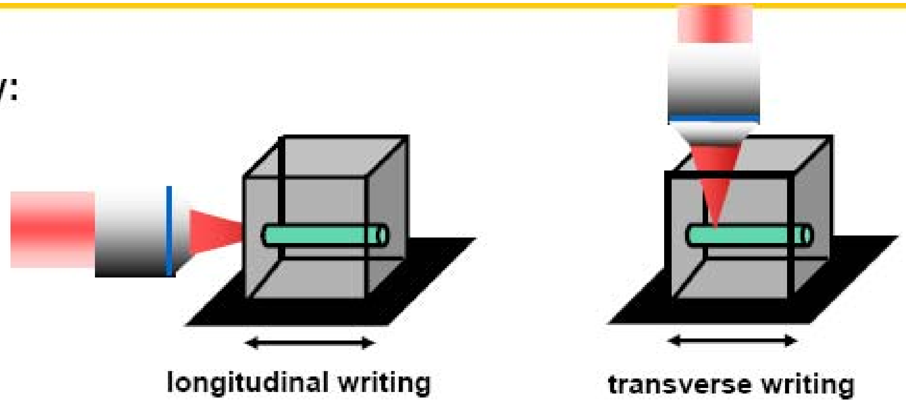

- pulse energy: 0.1-10 μJ:
- laser wavelength: 800 nm
- pulse repetition rate

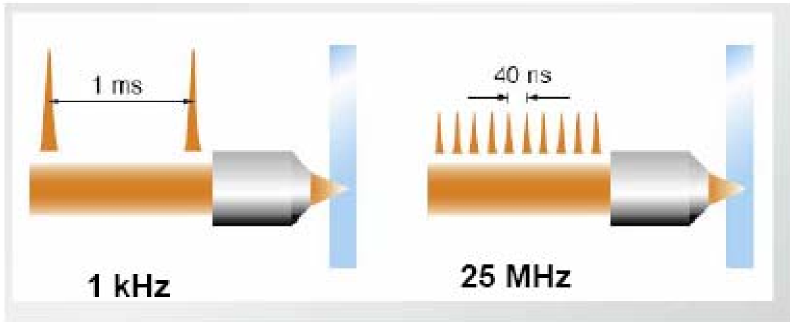

II.4 REDG planar and channel waveguides

C-band waveguide amplifier produced by femtosecond laser writing

G. Della Valle, R. Osellame, N. Chiodo, S. Taccheo, G. Cerullo, and P. Laporta

Istituto di Fotonica e Nanotecnologie del CNR – Dipartimento di Fisica del Politecnico di Milano P.zza L. da Vinci 32, 20133 Milano, Italy.
giuseppe.dellavalle@polimi.it

A. Killi and U. Morgner

Max-Planck-Institut für Kernphysik, Saupfercheckweg 1, D-69117 Heidelberg, Germany

M. Lederer and D. Kopf

HighQLaser Production GmbH, Kaiser-Franz-Josef-Str. 61, A-6845 Hohenems, Austria

8 August 2005 / Vol. 13, No. 16 / OPTICS EXPRESS 5976

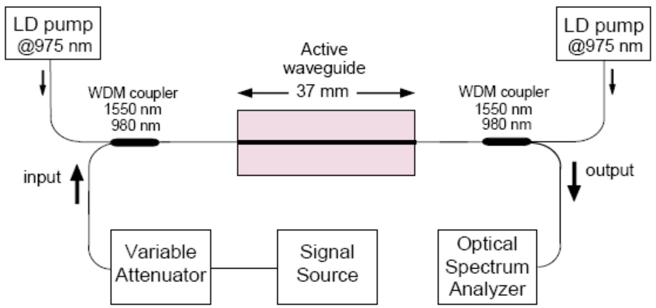

Fig.1. Optical waveguide amplifier configuration and characterization set-up.

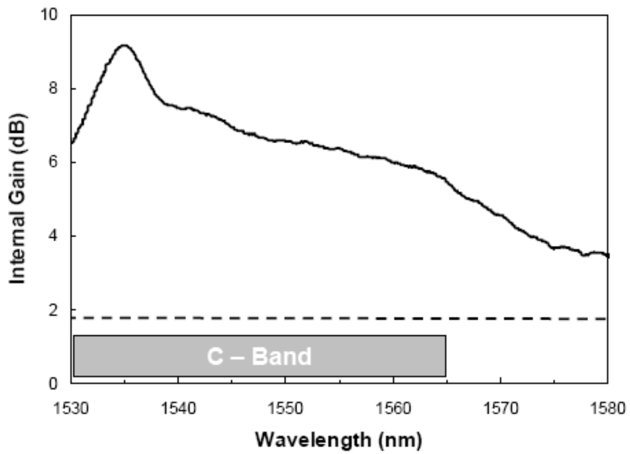

Fig. 2. Measured internal gain spectrum obtained with an incident pump power of 460 mW in bi-directional pumping configuration. The dashed line indicates the total insertion losses.

II.5 REDG microbarcodes

Rare earth-doped glass microbarcodes

Matthew J. Dejneka*, Alexander Streltsov, Santona Pal, Anthony G. Frutos, Christy L. Powell, Kevin Yost, Po Ki Yuen, Uwe Müller, and Joydeep Lahiri*

Science and Technology Division, Corning Incorporated, Corning, NY 14831

PNAS 2003;100;389-393; originally published online Jan 6, 2003;
doi:10.1073/pnas.0236044100

- Employs μm size glass barcodes
- UV excited fluorescences
- APPLICATION: Bioessays

Advantages of REDG

- High quantum efficiencies
- Noninterference with common fluorescence labels
- Inertness to most organics and aqueous solvents

> 10^6 distinguishable possibilities

II.5 REDG microbarcodes

Rare earth-doped glass microbarcodes

Matthew J. Dejneka*, Alexander Streltsov, Santona Pal, Anthony G. Frutos, Christy L. Powell, Kevin Yost, Po Ki Yuen, Uwe Müller, and Joydeep Lahiri*

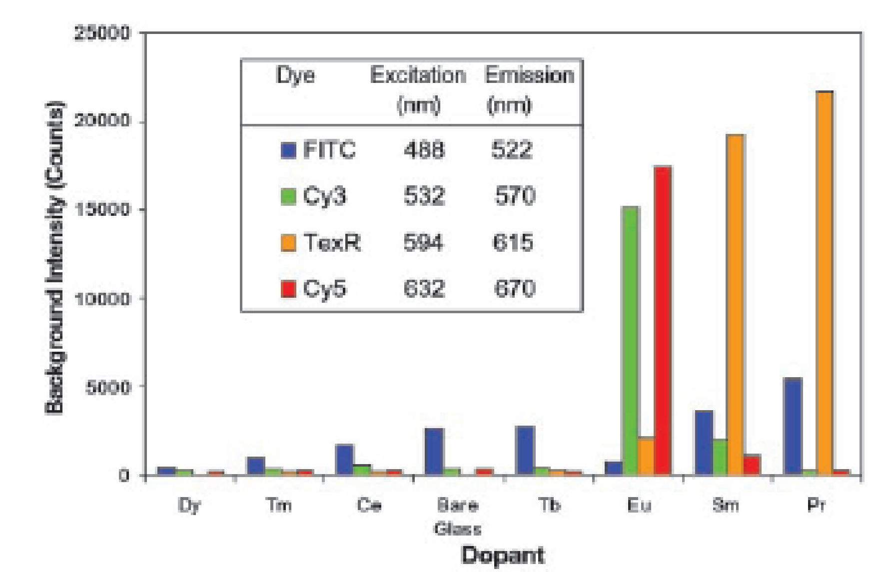

Fig. 2. Background fluorescence of RE-doped glasses relative to a bare microscope slide.

Fabrication of Barcodes. Conventional optical fiber draw methods were used to fabricate the encoded fiber ribbons. First, the optimized glasses were melted and cast into 25 × 25 mm square bars and annealed for 1 h at 750°C. These bars were drawn into lengths of square (3.5-mm sides) canes and stacked in a predetermined order to define a barcode pattern. The assembly was then fused in a graphite press in a furnace at 900°C under N_2. The fused preform was drawn at 1,200°C into a ribbon fiber (20 μm thick, 100 μm wide). The ribbon fiber was scribed every 20 μm at a rate of 5 mm/s with 800-nm femtosecond laser pulses (100 mW average power) by using a computer-controlled stage. The scribed ribbon fiber was then sonicated for 60 s in water to break the ribbon along the scribes into individual barcodes.

II.5 REDG microbarcodes

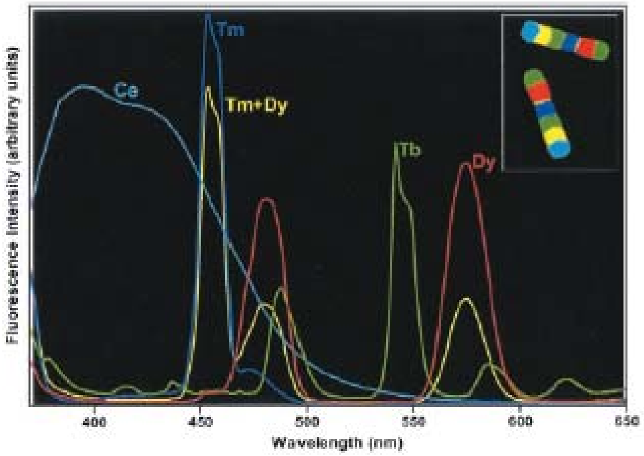

Fig. 3. False-color image of two 100 × 20 μm barcodes (*Inset*) and corresponding fluorescence spectrum barcode elements. The same color scheme is used for the spectra and the image [e.g., the yellow band in the barcode corresponds to the yellow (combination Tm+Dy) line spectrum].

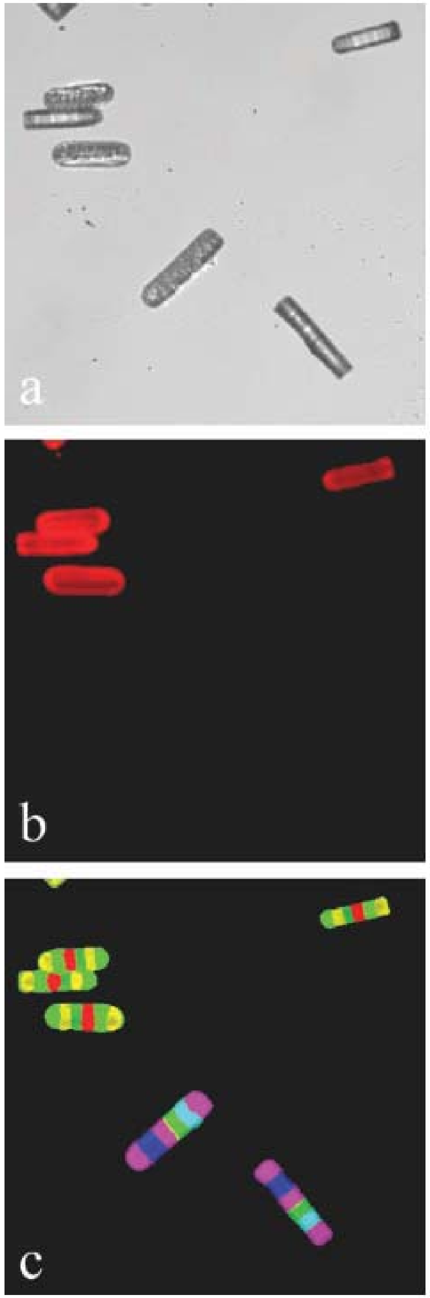

Fig. 4. Fluorescence false-color images of barcode particles A and B used in a DNA hybridization assay using Cy3-labeled DNA. (*a*) "White light" image. (*b*) Cy3 channel image. (*c*) RE images obtained by using a 420-nm long-pass filter.


Break time!!!!!!